Search for Higgs bosons of minimal supersymmetry: Impact of supersymmetric decay modes

Howard Baer
Department of Physics, Florida State University, Tallahassee, Florida 32306

Mike Bisset
Department of Physics and Astronomy, University of Hawaii, Honolulu, Hawaii 96822

Duane Dicus
Center for Particle Physics, University of Texas, Austin, Texas 78712

Chung Kao
Department of Physics, Florida State University, Tallahassee, Florida 32306

Xerxes Tata
Department of Physics and Astronomy, University of Hawaii, Honolulu, Hawaii 96822
(Received 20 July 1992)

We investigate the prospects for the detectability of the Higgs bosons of the minimal supersymmetric model (MSSM) at future colliders. First we delineate regions of MSSM parameter space where the various Higgs bosons may be observable at the CERN e^+e^- collider LEP 200 or hadron supercolliders, assuming (as usual) that Higgs-boson decay modes to supersymmetric particles are not allowed. We find that, even with optimistic assumptions of detector capabilities, there exist regions of parameter space where none of the Higgs bosons are visible. Next, we show that there are substantial regions of parameter space where rates for Higgs-boson decays to supersymmetric particles are large, and even dominant. These decays reduce the rates for conventional Higgs-boson signatures, thus making conventional detection of Higgs bosons even more difficult. However, a number of new, promising modes for Higgs-boson detection have opened up. These include a "gold-plated" Higgs scalar or pseudoscalar decay to four leptons plus missing energy which may make possible a precise mass measurement of the lightest and second lightest neutralino. Furthermore, rare decays of the top quark into a b quark plus three leptons may be visible, and signal charged-Higgs-boson decays to a chargino plus neutralino.

PACS number(s): 14.80.Gt, 12.10.Dm, 13.85.Qk, 14.80.Ly

I. INTRODUCTION

The need to unravel the mechanism for the spontaneous breakdown of electroweak symmetry is one of the main reasons for exploring the TeV energy scale at, for instance, hadron supercolliders such as the Superconducting Super Collider (SSC) in the United States and the Large Hadron Collider (LHC) in Europe. In the standard model (SM) the breaking of electroweak symmetry is realized by introducing a doublet of spin-0 fields which acquires a nonzero value in the ground state. A scalar particle, the Higgs boson, is a relic of this method of breaking the symmetry and can be searched for at colliding beam facilities [1]. The nonobservation of a signal [2] for Higgs bosons produced via $Z \to Z^* + H_{\rm SM}$ in the experiments at the CERN e^+e^- collider LEP has been translated to a lower bound,

$$m_{H_{\rm SM}} > 57 \text{ GeV}, \tag{1}$$

on the mass of the SM Higgs boson, where $H_{\rm SM}$ is the physical Higgs boson of the SM.

The fact that the scalar sector of the SM is unstable to radiative corrections that arise when the SM is coupled to ultraheavy degrees of freedom as, e.g., in a grand unified theory, has led many authors to seriously consider various alternatives. One such alternative is supersymmetry (SUSY) which is the only known symmetry that can maintain the stability of the scalar symmetry-breaking sector [3], provided only that the superpartners of the known particles are not much heavier than ~ 1 TeV. The search for these sparticles and the development of new strategies to find them has been the subject of much theoretical [4] and experimental [5] activity in recent years.

Unlike in the SM, the Higgs sector of any supersymmetric theory contains at least two SU(2) doublets [6]. Within the minimal supersymmetric model (MSSM)[7] the Higgs sector is completely specified by just two doublets h and h' that couple to the $T_3 = \frac{1}{2}$ and $T_3 = -\frac{1}{2}$ fermions, respectively. The physical particles, therefore, consist of two neutral scalars, H_l and H_h ($m_{H_l} < m_{H_h}$), one pseudoscalar (H_p), and a pair of charged bosons ($H^\pm$). (In this paper, we let H with no subscript denote a generic Higgs boson.) At the tree level, the masses and couplings of all these particles are completely determined [6] by $\tan\beta = \frac{v}{v'}$ and the mass of any one of the bosons, which we take to be m_{H_p}.

Several groups have pointed out that if the top quark is heavy, radiative corrections from the large t-quark Yukawa coupling substantially modify the tree-level formulas for masses and mixing patterns in the Higgs sector [8]. This has important implications for MSSM Higgs boson (as well as other sparticle) searches at LEP. For instance, the nonobservation of any signal from MSSM Higgs bosons at LEP [9] can no longer be used to infer any limit on $\tan\beta$, since the tree-level inequality, $m_{H_l} < |M_Z \cos(2\beta)|$, on which this bound is based, is significantly altered.

The region of the m_{H_p} vs $\tan\beta$ parameter plane of the MSSM Higgs sector excluded by the negative results [9] of the experiments at LEP is shown in Fig. 1. In our analysis, we have incorporated the effects of radiative corrections due to top-quark Yukawa interactions [8] using the formulas in Ref. 10. We have used the limit (1) on the mass of the SM Higgs boson to infer an upper limit on the production of H_l via $Z \to Z^* + H_l$, taking into account the differences in the couplings of H_l and $H_{\rm SM}$. The MSSM Higgs bosons can also be produced via $Z \to H_l + H_p$, which proceeds via gauge interactions. We have assumed that the nonobservation of this two-body decay in the total sample of about 2×10^6 Z events at LEP can be used to infer that $m_{H_l} + m_{H_p} > M_Z$ [11]. It is interesting to see that already the LEP experiments exclude $m_{H_p} < 40$ GeV, regardless of m_t or $\tan\beta$. Within our framework, this corresponds to $m_{H^+} > 90$ GeV, which essentially excludes the possibility of seeing H^+ signals at LEP 200. Finally, we have also shown the region of this plane that might be probed at LEP 200. Following Ref. [12], we have made both optimistic and conservative projections of the reach during this second

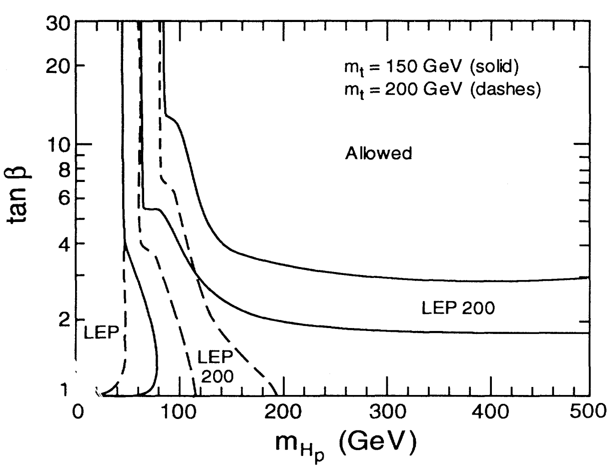

FIG. 1. Regions in the m_{H_p}-$\tan\beta$ plane which are excluded by Higgs-boson searches at LEP, for the decays $Z \to H_p H_l$ and $Z^* H_l$. We show excluded regions for $m_t = 150$ (solid) and 200 GeV (dashed). We also show the conservative and optimistic contours for regions explorable at LEP 200. The LEP 200 criteria are given in the text.

phase of LEP. For the former, we have assumed $\sqrt{s} = 190$ GeV and taken 0.05 pb as the lower limit for an observable cross section for either the $e^+e^- \to ZH_l$ or the $e^+e^- \to H_l H_p$ processes. The conservative estimate assumes $\sqrt{s} = 175$ GeV and a lower limit of 0.2 pb on the cross sections. It is interesting to note that even at LEP 200 a nonobservation of any Higgs-boson signal cannot be used to infer any bound on $\tan\beta$, at least for the case of a very heavy top quark.

The nonobservation of sparticles in Z decays at LEP further constrains the parameter space of the MSSM. We remind the reader that within this framework the masses and relevant couplings of all sparticles are fixed in terms of just a few additional parameters which we may take to be (i) the gluino mass, $m_{\tilde{g}}$ (which, we assume, derives from a common gaugino mass at the unification scale, and hence, also fixes the SU(2) and U(1) gaugino masses), (ii) a common mass ($m_{\tilde{q}}$) for all the sfermions, and (iii) a supersymmetric Higgsino mixing mass $2m_1 = -\mu$, which along with $m_{\tilde{g}}$ and $\tan\beta$ determines the chargino ($\widetilde{W}_i$) and neutralino ($\widetilde{Z}_i$) masses and mixing patterns. The precise measurement of the Z width $\Gamma_Z = 2.487 \pm 0.010$ [13] together with the SM lower bound [14], $\Gamma_Z > 2.468$ GeV leads to a 95% C.L. upper bound on the contribution of new particles to the Z width:

$$\Delta\Gamma_Z < 35 \text{ MeV}. \tag{2a}$$

Similarly, the measurement [13] of the invisible width of the Z, Γ_Z (invisible) $= 498 \pm 8$ MeV, leads to the bound

$$\Delta\Gamma_Z \text{ (invisible)} < 11 \text{ MeV}. \tag{2b}$$

While (2a) limits the production of all sparticles that couple to the Z, (2b) serves to restrict the rate for the decay of the Z to a pair of lightest supersymmetric particles (LSP), which we assume will escape detection [4, 7]. We take the LSP to be the lightest neutralino ($\widetilde{Z}_1$). Further restrictions come from the negative outcome of searches for charginos [15] and neutralinos [16] (other than $\widetilde{Z}_1$ pairs). The large coupling of the charginos to Z essentially requires that [17]

$$m_{\widetilde{W}_1} > 45 \text{ GeV}, \tag{2c}$$

while the published results of the LEP experiments [16] based on an analysis of just $\sim 10^4$ Z decays limit the branching fraction for the decays, $Z \to \widetilde{Z}_1\widetilde{Z}_2$ and $\widetilde{Z}_2\widetilde{Z}_2$ to be smaller than a few times 10^{-4}. In view of the vastly larger sample of Z's available today, we have required that the branching fraction for the decays $Z \to \widetilde{Z}_i\widetilde{Z}_j$ (where i and j are not both 1) satisfies

$$B(Z \to \widetilde{Z}_i\widetilde{Z}_j) < 5 \times 10^{-5}. \tag{2d}$$

Since the masses and couplings of $\widetilde{W}_i$ and $\widetilde{Z}_j$ are fixed by the parameters, $m_{\tilde{g}}$, μ, and $\tan\beta$, the constraints (2a)–(2d) exclude the region of the $m_{\tilde{g}}$-μ plane shown in Fig. 2 [18]. Also shown by the dashed line labeled CDF (Collider Detector at Fermilab Collaboration) is the direct limit on the gluino mass from the nonobservation [19] of an excess of $\not{E}_T$ events from the production of gluino

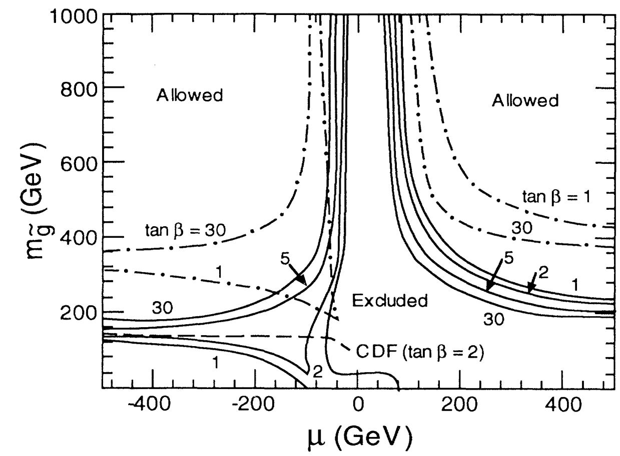

FIG. 2. Regions in the μ-$m_{\tilde{g}}$ plane, which are excluded by measurements of Z decay properties at LEP, for various values of $\tan\beta$ (solid curves). Also shown by a dashed line is the CDF constraint (modified for cascade decays for $\tan\beta = 2$) due to lack of missing energy signals in $p\bar{p}$ collisions. The dot-dashed curves are contours for $m_{\widetilde{W}_1} = 90$ GeV for two values of $\tan\beta$ and correspond to the approximate reach of LEP 200.

pairs at the Fermilab Tevatron, with the effect of cascade decays of the gluinos incorporated [20]. We have not shown this for positive values of μ, since the LEP results essentially exclude the whole region that could be probed at the Tevatron for all values of $\tan\beta$. Finally, we have also shown by dot-dashed lines the contours of $m_{\widetilde{W}_1} = 90$ GeV for two extreme values of $\tan\beta$. This represents the region of parameter space that might be probed at LEP 200.

We see from Fig. 1 that there is a large part of the parameter space that will not be probed even during the second phase of LEP. Indeed if the parameters are in this range, the Higgs bosons will have to be searched for at other facilities such as higher-energy e^+e^- colliders or at hadron supercolliders such as the SSC and the LHC that are expected to become operational around the turn of the century. Already much effort [10, 12, 21–27] has been devoted to the study of the prospects for being able to search for MSSM Higgs bosons at hadron supercolliders. The observation that even H_l may be beyond the kinematic reach of LEP 200 has provided additional impetus to these studies. Although an assessment of these studies forms the subject of the next section, we mention here that the common result of all the analyses [10, 12, 21] is that there are ranges of $(m_{H_p}, \tan\beta)$ for which there is no observable signal for any of the Higgs bosons, at LEP 200 or at hadron supercolliders.

Most studies of the signals from MSSM Higgs bosons assume that these cannot decay into other sparticles. Whereas this may be natural to assume for H_l, we see no reason why this should be so for H_h, H_p, and $H^{\pm}$. Since model calculations show that the lighter charginos and neutralinos may have masses smaller than or close to intermediate vector boson masses, the decays of Higgs bosons into these may be especially important. If these decays are kinematically accessible, they are often the dominant decay modes, particularly if the decays to t quarks are kinematically forbidden. This is because H_p does not couple to vector-boson pairs at the tree level, whereas the coupling of these to H_h is strongly suppressed by mixing angle factors, especially for larger values of m_{H_h}. Even for H_l, the decay $H_l \to \widetilde{Z}_1\widetilde{Z}_1$ can be significant [28] although for a limited range of SUSY parameters.

The SUSY decays of Higgs bosons are important for two reasons. First, their presence can greatly reduce the SM decay modes of the Higgs bosons, thereby reducing the size of the conventional signals via which they might be detectable at the SSC or the LHC. This can be especially important for rare decays of Higgs bosons (such as via the $\gamma\gamma$ mode) for which the signal is already small. On the positive side, however, the decays of Higgs bosons into charginos and neutralinos may lead to new channels for Higgs boson detection. A study of the impact of SUSY decays of Higgs bosons on their detection at the SSC and/or LHC forms the main subject of this paper.

The remainder of this paper is organized as follows. In Sec. II, we review various strategies that have been proposed for Higgs-boson searches at hadron supercolliders and present our own assessment of the region of parameter space that can be probed at hadron supercolliders, assuming that sparticles are too heavy to be produced in Higgs boson decays. In Sec. III, we map out the regions of SUSY parameters, where the decays of Higgs bosons into charginos and neutralinos may be significant, and then study how these new decay modes impact on the signals studied in Sec. II (and much of the literature). In Sec. IV we assess prospects for detecting the MSSM Higgs bosons via their SUSY decay modes. We conclude in Sec. V with some general remarks and a summary of our results.

II. SEARCH STRATEGIES FOR MSSM HIGGS BOSONS

Many of the important signatures of MSSM Higgs bosons are the same as those for the SM Higgs bosons [1, 6]. However, in the MSSM, there are essential differences that arise from additional "mixing angle factors" that are absent in the SM.

These mixing angle factors may enhance certain decay modes (e.g., $H_p \to b\bar{b}$, for large values of $\tan\beta$), while reducing others (e.g., $H_h \to ZZ$, for large values of m_{H_p}) from their SM expectation. As in the case of $H_{\rm SM}$, the optimal strategy to search for MSSM Higgs bosons at hadron colliders depends on the parameters of the Higgs sector (in the SM case only on $m_{H_{\rm SM}}$). We will briefly review these and then present the results of our analysis of the region of parameter space that might be probed at the SSC and the LHC, assuming that SUSY decays of all the Higgs bosons are highly suppressed.

As mentioned in Sec. I, we have incorporated the effects of radiative corrections from t-quark Yukawa interactions in our analysis. The relevant assumptions and formulas for masses and mixing angles may be found in

Ref. [10] and will not be repeated here. In this paper we have, however, also included correction terms of order $\sim [\frac{m_t^4}{M_W^4}\ln(1+\frac{m_{\tilde{t}}^2}{m_t^2})]$ to triple Higgs-boson couplings (the corrections to other vertices such as HWW, etc., do not grow as m_t^4/M_W^4), again within the effective potential approximation. We will see below that these corrections can significantly alter the partial width for the H_lH_l and H_pH_p decays of the heavier Higgs bosons, and, thus, the branching fractions for the experimentally interesting decays. We have checked that, with the replacement $\alpha \to -\alpha$ (which arises from a difference of conventions) and the splitting of the log terms as in (3b) below, to take into account a possible mass splitting between $\tilde{t}_R$ and the $(\tilde{t}_L, \tilde{b}_L)$ doublet, our results are in agreement with Eqs. (25)–(27) of Ref. [12]. For brevity, we write here the coupling constant only for the $H_hH^+H^-$ vertex as this was not included in Ref. [12]. In the notation of Ref. [10], we find

$$\mathcal{L} \ni \lambda H^+H^-H_h\ , \tag{3a}$$

with,

$$\lambda = -gM_W\left[\cos(\alpha+\beta) - \frac{1}{2}\frac{\cos(\beta-\alpha)\cos(2\beta)}{\cos^2\theta_W} - \frac{3}{32\pi^2}\frac{g^2m_t^4}{M_W^4}\frac{\sin\alpha}{\sin\beta}\cot^2\beta\ln\left\{\left(1+\frac{m_{\tilde{t}_R}^2}{m_t^2}\right)\left(1+\frac{m_{\tilde{L}}^2}{m_t^2}\right)\right\}\right]. \tag{3b}$$

We note that the $H_lH^+H^-$ vertex can be simply obtained by the replacements $\sin(\alpha) \to -\cos(\alpha)$ and $\cos(\alpha) \to \sin(\alpha)$.

Turning to the detection prospects for the Higgs boson, we will, as in Ref. [10], make optimistic (but technically possible) assumptions about the detector. Our goal is to delineate the range of MSSM parameters for which Higgs-boson detection may or may not be possible even under optimal conditions. We begin by considering various final states in turn.

A. $H \to ZZ$

The decay $H \to ZZ$ (where both Z bosons decay to e's or μ's) provides the "gold-plated" signature via which it is possible to search for a SM Higgs boson as heavy as about 800 GeV. In the case of the MSSM, this is no longer the case because, as m_{H_p} (and hence, m_{H_h}) gets very large, H_h decouples from the vector boson pairs, while H_l couples to these in the same way as $H_{\rm SM}$. H_p, of course, has no tree-level coupling to W or Z pairs so that its detection via the ZZ mode (which occurs via one-loop effects) may be feasible only for very special values of SUSY parameters [24]. In our analysis, we have ignored the possibility of detecting $H_p \to ZZ$ decays, and focused on the possibility of detecting the neutral scalars in the $4l$ ($l = e$ or μ) channel (including decays where one of the Z bosons may be virtual). We have included a detection efficiency of 0.35 [23] in our computation of the $4l$ signal. We have further required that the four leptons reconstruct the mass of the parent Higgs boson within a resolution Δm given by

$$\Delta m(4l) = 2.2\text{ GeV} + 0.0145 \times [m(4l) - 200]\text{ GeV}, \tag{4}$$

which although optimistic, is technically feasible [23].

For $m_H > 2M_Z$, the dominant background to the $4l$ signal comes from the continuum pair production of leptonically decaying Z''s by $q\bar{q}$ and gg fusion (via loops) [29] where the $m(4l)$ accidently falls into the "signal region" $m_H \pm \Delta m$ (which, because of the narrowness of the Higgs boson, is all confined to within Δm about m_H). For 125 GeV $< m_H < 2M_Z$, the signal comes from ZZ^* decays, while ZZ^* and $Z\gamma^*$ are the main backgrounds. It has been shown [30] that the continuum production of ZZ^* is essentially negligible and the continuum $Z\gamma^*$ contribution to the $4l$ background [which peaks sharply at $m(\gamma^*) = 0$] can be removed by imposing a mass cut on the dileptons from the virtual photon, provided that $m(Z^*)$ in the signal is not too small. We consider the $4l$ signal to be of interest only if $m_H > 125$ GeV [31].

As in Ref. [10], we define the signal to be observable if the 99% confidence level upper limit on the background is smaller than the corresponding lower limit on the signal plus background so that

$$L(\sigma_s+\sigma_b) - 2.32\sqrt{L(\sigma_s+\sigma_b)} > L\sigma_b + 2.32\sqrt{L\sigma_b}, \tag{5}$$

where L is the integrated luminosity, and σ_b is the background cross section within a bin of width $\pm\Delta m$ centered at m_H. Note that while this reduces to the usual measure of the statistical significance $\frac{L\sigma_s}{\sqrt{L\sigma_b}}$ when the background is much larger than the signal, (5) is rather different in the more general case. Finally, we remark that we have not considered the $H \to WW$ mode, which is feasible for the detection of SM Higgs bosons. The suppression of the cross section due to mixing-angle factors makes the 2 jet $+\,l$ mode more difficult to detect over quantum-chromodynamics (QCD) backgrounds.

B. $H \to \gamma\gamma$

For Higgs bosons in the intermediate mass range, the $\gamma\gamma$ decay mode provides a promising way to detect the signal. We assume a mass resolution of $\pm 1\%$ for the $\gamma\gamma$ system (the analysis of Ref. [32] suggests that this is certainly feasible for the gamma-electron-muon (GEM) detector at the SSC, regardless of whether BaF_2 or liquid-argon calorimeters are used). Except for the incorporation of radiative corrections to the trilinear Higgs-boson vertices, our analysis of the $\gamma\gamma$ signal and background parallels that of Ref. 10, to which we refer the reader for further details. We mention, though, that the inclusion of these radiative corrections can have a substantial effect, especially when $\tan\beta$ is close to unity. In particular, the rate for the decay $H_h \to H_l H_l$ can change by large factors, resulting in corresponding enhancement or suppression of the various promising H_h decay modes.

We also note that the production of a Higgs boson in association with a W has been suggested [33] as a possible way of detecting the intermediate mass Higgs boson via the $l\gamma\gamma$ final state. It has been argued that even for the MSSM this process results in a higher signal-to-background ratio [12, 21]. The small number of events (after cuts to remove backgrounds) leaves very little margin for error on its normalization. In addition, there may be several reducible sources of background which have been considered only at the parton level [12, 21]. In contrast, because of the smooth continuum background that is present for the $\gamma\gamma$ signal, uncertainties in the background arising from unknown QCD corrections or incomplete knowledge of the structure functions will be irrelevant, since data on photon pairs outside the region of the Higgs bump will be bountiful.

C. $t \to bH^+$

If the top quark is heavy as it now appears to be [34], the decay $t \to bH^+$, if kinematically accessible, may provide [12, 21, 35–37] yet another handle on the Higgs sector of the MSSM. For $\tan\beta \gtrsim \frac{3m_b^2}{m_\tau^2} \sim 1-2$, H^+ dominantly decays via $H^+ \to \tau\nu$, so that its production via t-quark decays is signaled by an excess of τ leptons over and above the rate expected from the usual decay chain $t \to bW$, $W \to \tau\nu$. The quantity $R_{\tau l}$ defined by

$$R_{\tau l} = \frac{B(t \to \tau\nu_\tau b)}{B(t \to l\nu_l b)} = 1 + \frac{B(t \to H^+ b)B(H^+ \to \tau\nu_\tau)}{B(t \to Wb)B(W \to l\nu_l)} = 1 + \Delta R_{\tau l} \tag{6a}$$

(where $l = e$ or μ) is expected to be unity in the SM so that its deviation $\Delta R_{\tau l}$ serves as a measure of the charged Higgs-boson decay mode of the t quark. The τ's are supposed to be identified via their hadronic decays. This has been carefully studied for the LHC [35] by starting with a sample of tagged $t\bar{t}$ events (defined by an $e\mu$ sample with $p_T(e) > 75$ GeV and $p_T(\mu) > 25$ GeV from the same top quark) and determining the ratio of the N_τ/N_μ of the number of decays where the other t quark in the $t\bar{t}$ pair decays into a μ or a τ. We can then write [35]

$$R_{\tau\mu} = A\frac{N_\tau}{N_\mu} + B, \tag{6b}$$

where

$$A = \frac{\epsilon_{W\to\mu}}{B(\tau \to \text{hadrons})\epsilon_{H^+\to\tau}} \tag{6c}$$

and

$$B = 1 - \frac{\epsilon_{W\to\tau}}{\epsilon_{H^+\to\tau}}. \tag{6d}$$

Here $\epsilon_{\ldots}$ is the experimental efficiency for the detection of the particular process. It is then easy to check that the variance of R is given by $A^2 N_\tau \frac{(N_\tau + N_\mu)}{N_\mu^3}$. For $m_t = 200$ GeV, Felcini [35], via a simulation of 2389 tagged $t\bar{t}$ events corresponding to an integrated luminosity of 10 fb^{-1} at the LHC, has estimated that $\epsilon_{W\to\mu} = 94\%$ and $\epsilon_{W\to\tau}B(\tau \to \text{hadrons}) = 35\%$ and, further, that for $m_{H^+} = 150$ GeV, $\frac{\epsilon_{H^+\to\tau}}{\epsilon_{W\to\tau}} = 1.5$. Since R is not distributed as a Gaussian, we obtain a criterion for observability of the $t \to bH^+$ signal at the LHC, assuming an integrated luminosity of 10 fb^{-1} by requiring that $R_{\tau\mu}$ deviates from its SM value of unity by at least four times the variance which, for the above choice of parameters, yields an observable signal if $\frac{\Delta R_{\tau\mu}}{R_{\tau\mu}} > 0.32$. Several remarks are in order.

(1) There are additional systematic uncertainties from errors on tracking efficiency (which affects the number of detected charged tracks) and energy resolution of the calorimeter, both of which can affect the number of detected τ's which have not been taken into account.

(2) Obviously, the efficiency of τ detection decreases with m_{H^+}, so that if H^+ is considerably lighter, the τ detection efficiency may have been considerably overestimated.

While we are aware that spin effects favor a harder pion spectrum from the decays of τ's in H^+ decays (as compared to W^+ decays), and, hence, a higher detection efficiency, we have [in view of additional uncertainties (1) and (2), above] conservatively taken $\frac{\epsilon_{H^+\to\tau}}{\epsilon_{W\to\tau}} = 1$ in our analysis. In this case, the expression for the fractional variance of $R_{\tau\mu}$ simply reduces to $\sqrt{\frac{1}{N_\mu} + \frac{1}{N_\tau}}$. In the SM, $N_\mu \sim 250$, $N_\tau \sim 100$ for tagged top events per 10 fb^{-1} at the LHC, so that our requirement for a detectable signal at the LHC reduces to

$$\Delta R_{\tau\mu} > 0.48 \qquad [\text{LHC},\ 10\ \text{fb}^{-1}]. \tag{7a}$$

We assume similar detection efficiencies at the SSC, since these are fixed by the event kinematics (and so are more sensitive to the particle masses than the machine energy). Thus, N_μ and N_τ are increased in proportion to the increase in the $t\bar{t}$ cross section so that at the SSC we require (after scaling by the square root of the number of events)

$$\Delta R_{\tau\mu} > 0.2 \qquad [\text{SSC},\ 10\ \text{fb}^{-1}]. \tag{7b}$$

For the LHC operating at the design luminosity of 100 fb^{-1}/yr, the ten times larger $t\bar{t}$ sample implies that

$$\Delta R_{\tau\mu} > 0.15 \qquad [\text{LHC},\ 100\ \text{fb}^{-1}] \tag{7c}$$

would be observable. In view of the simplicity of our estimates, we will take (7b) to be the limit of observability both at the SSC and at the LHC.

D. $H \to \tau\bar{\tau}$

It has also been suggested [12] that it may be possible to search for the neutral Higgs bosons H_h and H_p via their decays to τ pairs. This is especially interesting because the detection of $\gamma\gamma$ pairs from H_p (which is one of the few promising ways to search for it) appears feasible only if $\tan\beta$ is close to unity [10]. The continuum production of Drell-Yan τ pairs is an obvious background, since the neutrinos preclude the possibility of looking for a $\tau\bar{\tau}$ mass bump. It has, however, been pointed out [38] that for relativistic τ pairs recoiling against hard jets, the kinematics of the event is sufficiently constrained to allow for a measurement of $m(\tau\bar{\tau})$ with a precision of about 15%. For $H_{\rm SM}$, this was studied in Ref. [39], where the τ pairs were detected via the $e\mu$ mode. It was concluded that leptonic decays of the top quark posed a formidable background for $H_{\rm SM}$ detection.

Based on the fact that the cross section for the production of H_p (H_h) may exceed that for $H_{\rm SM}$ by a factor of up to about 30 (7), Kunszt and Zwirner have suggested that it may be possible to detect H_p or H_h via their decays to τ pairs. It should, however, be remembered that only high p_T Higgs bosons, i.e., those produced in association with jets, are detectable by this method, so that the useful cross section will be considerably smaller than the total cross section for H_h or H_p production. A very interesting possibility for H_p detection might be to study $H_p \to Z + H_l$ (which generally has a large branching fraction if it is kinematically allowed) followed by $H_l \to \tau\bar{\tau}$. The high p_T Z then serves to provide the recoil needed for a measurement of the $\tau\bar{\tau}$ mass. Furthermore, since the Z is produced by a two-body decay of H_p, its p_T distribution is expected to show a characteristic Jacobian peak. We are currently investigating the feasibility of this method as well as of the detectability of the $H_p, H_h \to \tau\bar{\tau}$ mode. Since a careful study is needed before any signal can be claimed, we will conservatively not include this in the analysis presented in the rest of this paper.

E. Numerical results

We now turn to a study of the regions of the m_{H_p}-$\tan\beta$ plane, where the $\gamma\gamma$ or $4l$ decays of MSSM Higgs bosons lead to observable signals at the SSC and/or LHC, assuming the criteria for observability described above. In addition to these, we have required a minimum of 10 (25) signal events for an integrated luminosity of 10 fb^{-1} (50 or 200 fb^{-1}). We have fixed $m_{\tilde{g}} = -\mu = 1$ TeV for the remainder of this section to ensure that the charginos and neutralinos are all heavy. Although this is not sufficient to kinematically close all the SUSY channels, our choice of parameters ensures that the SUSY branching fractions are negligible. To see this, we recall that the $H\widetilde{W}_i\widetilde{W}_j$ or $H\widetilde{Z}_i\widetilde{Z}_j$ couplings occur only via Higgs-boson–Higgsino–gaugino interactions. For the very large choice of $|\mu|$, the lighter $\widetilde{W}_i$ and $\widetilde{Z}_j$ have very suppressed Higgsino components, so that the couplings of the Higgs bosons to $\widetilde{W}_1$, $\widetilde{Z}_1$, and $\widetilde{Z}_2$ are strongly suppressed.

The regions of the m_{H_p}-$\tan\beta$ plane, where the $\gamma\gamma$ (solid contours) or the $4l$ (dashed contours) signal is detectable at the SSC are shown in Fig. 3 (Fig. 4) for $m_t = 150$ GeV (200 GeV) and for an integrated luminosity of (a) 10 fb^{-1} (corresponding to one year of operation of the SSC at its design luminosity), and (b) 50 fb^{-1}. Also shown in these figures is the region already excluded by the LEP constraints discussed in Sec. I (solid contour) as well as our optimistic estimate of the region that might be probed at LEP 200 (dot-dashed contour). Unless otherwise denoted by an arrow, the labels are *inside* the region where the signal is detectable. Several features are worth noting.

(1) For $m_t = 150$ GeV, even with our optimistic assumptions about the capabilities of LEP 200 as well as of the $\gamma\gamma$ mass resolution that might be available at supercollider detectors, we see from Fig. 3 that there is a region (shaded) of large $\tan\beta$ around $m_{H_p} = 120$ GeV,

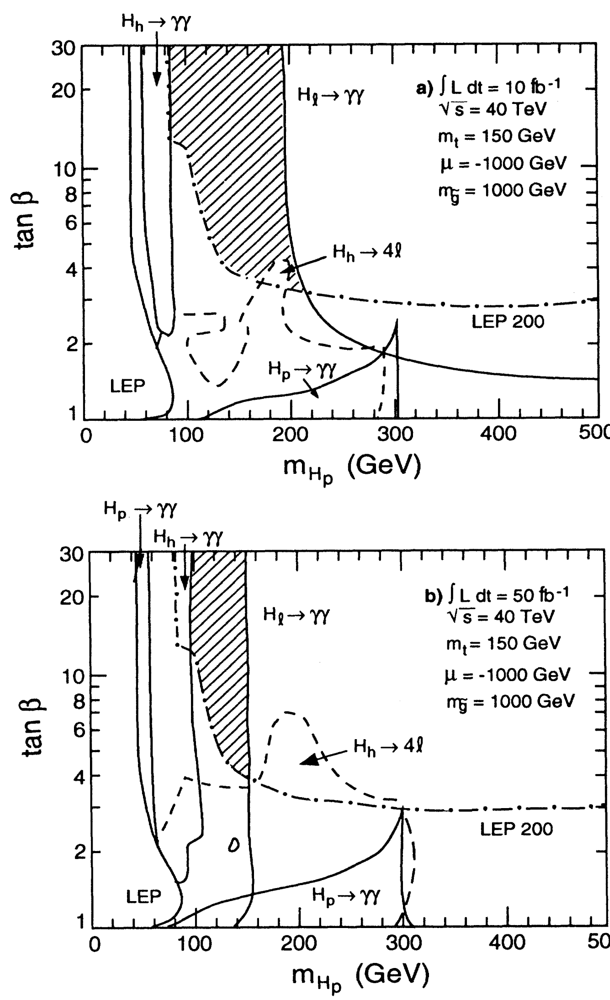

FIG. 3. Regions in the m_{H_p}-$\tan\beta$ plane, which are explorable via Higgs searches at the SSC. The region currently excluded by LEP as in Fig. 1 is indicated by a solid contour. Regions explorable via searches for $\gamma\gamma$ events are also indicated by solid contours; reaction labels are located *within* the explorable region, unless otherwise marked by an arrow. Regions explorable via gold-plated $4l$ signals are indicated by dashed contours. Finally, the region explorable by LEP 200 are indicated by dot-dashed contours. The shaded region is where none of the Higgs bosons of supersymmetry are visible by any of the considered signals. We take $m_t = 150$ GeV; other parameters are listed on the figure. We show plots for (a) integrated luminosity of 10 and (b) 50 fb^{-1}.

where there is no observable signal for *any* of the MSSM Higgs bosons either at LEP 200 or at the SSC, even after five years of operation.

(2) For $m_t = 150$ GeV, m_{H_l} is always smaller than 125 GeV so that the light scalar does not contribute to the $4l$ signal. For $m_t = 200$ GeV, however, $H_l \to 4l$ decays are observable over a large part of this plane and serve to fill a substantial portion of the hole where there was no observable signal for $m_t = 150$ GeV. In fact, as can be seen from Fig. 4(b), almost the complete parameter plane is covered by at least one signal after five years of operation of the SSC if $m_t = 200$ GeV.

(3) Amusingly, for $m_t = 150$ GeV, the $H_h \to 4l$ mode is observable only in those regions where there is at least one other detectable signal. For $m_t = 200$ GeV, however, there is a sizable portion of the plane where this is the only observable mode. It is interesting to note that for 100 GeV$< m_{H_p} <$ 140 GeV and large values of $\tan\beta$, H_h has large couplings to Z pairs, so that the branching fraction for the decay $H_h \to ZZ^*$ is actually larger (if m_{H_p} is in this range) than the real decay mode $H_h \to ZZ$

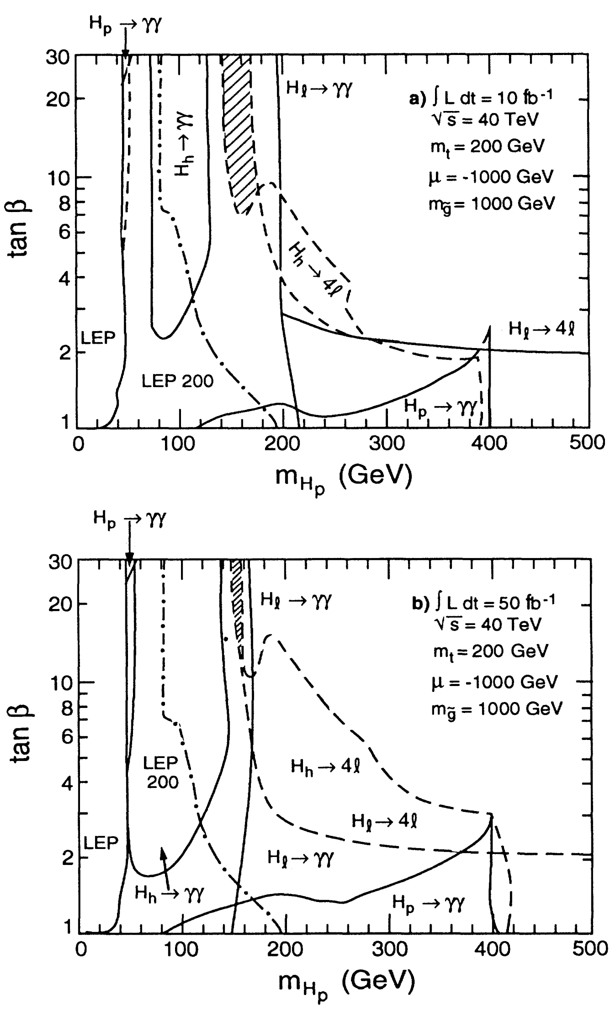

FIG. 4. Same as Fig. 3, except we have taken $m_t = 200$ GeV.

with $m_{H_h} \simeq 190$ GeV. This, together with the fact that the H_h production cross section falls with mass is why the region that can be probed via the $4l$ decay of H_h cuts off sharply as m_{H_p} is increased.

(4) There are several regions of parameter space where the signal from more than one of the Higgs bosons is observable. Simultaneous detection of two, or even all three, Higgs scalars would provide striking confirmation of a nonminimal Higgs sector.

The regions of parameter space that can be probed according to our criterion (7b) for the observability of the $t \to bH^+$ decays is to the left of the solid line in Fig. 5 for (a) $m_t = 150$ GeV, and (b) $m_t = 200$ GeV.

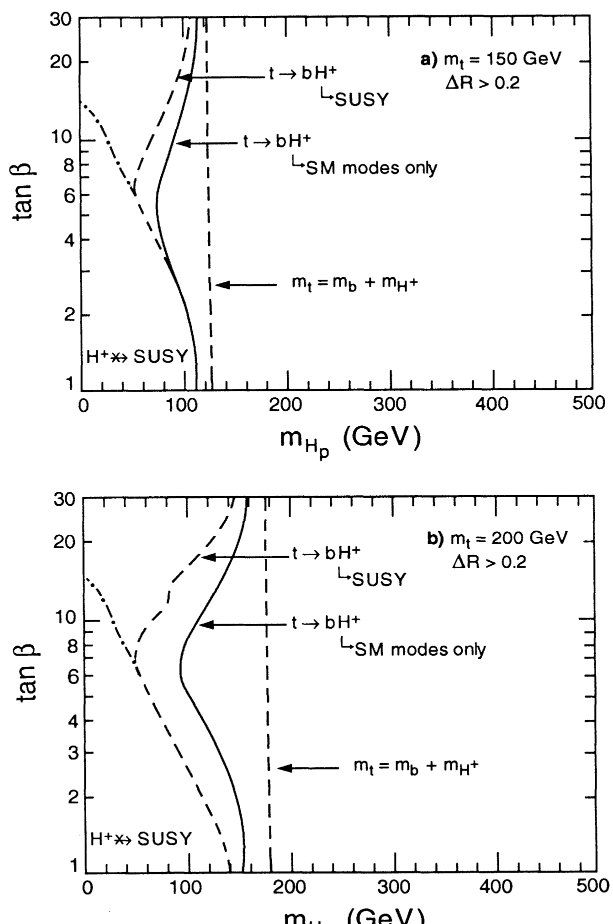

FIG. 5. Regions in the m_{H_p}-$\tan\beta$ plane, which are explorable via searching for $t \to bH^+$ followed by $H^+ \to \tau\nu$, for (a) $m_t = 150$ and (b) 200 GeV. The region to the left of the solid curve is where $\Delta R > 0.2$, where we have taken $m_{\tilde{g}} = 1000$ GeV, $\mu = 1000$ GeV, and $m_{\tilde{q}} = 1000$ GeV. If instead we take $m_{\tilde{g}} = 400$ GeV and $\mu = -70$ GeV, then SUSY decay modes of H^+ open up, and the charged Higgs boson is only discoverable to the left of the dashed region. The region to the left of the dot-dashed curve is where $H^+ \to SUSY$ particles are not allowed, even in the light SUSY parameter case above. We also show via the vertical dashed line the phase-space limit for $t \to bH^+$.

The vertical dashed curve denotes the kinematic limit for $t \to bH^+$ decays. The other curves show how this region is modified by the decays $H^+ \to \widetilde{W}_1 \widetilde{Z}_i$ of the charged Higgs boson, and will be further elaborated on in Sec. III. The range of m_{H^+} values that can be probed by looking for an excess of τ events is smallest for $\tan\beta \sim 6$. This reflects the fact that the product of branching ratios $B(t \to H^+ b)\, B(H^+ \to \tau\nu)$ has a minimum there [12, 21, 35–37]. Aside from reasons of clarity, we did not see fit to include these contours in Figs. 3 and 4 because it is clear that the arguments leading to (7b) are not at the same level of detail as those for the $\gamma\gamma$ or the $4l$ signal. We see that the $t \to bH^+$ decay can only fill in a small portion of the hole at very large values of $\tan\beta$, where our neglect [10] of the b-quark Yukawa coupling in the calculation of radiative corrections is likely to have the maximum impact. We should mention, though, that (7b) applies only for one year of SSC operation and that the observability limit on $\Delta R_{\tau\mu}$ would be reduced to 0.09 if the SSC were to be operated for five years. Finally, we note that it has been suggested that $t \to bH^+$ decays may also be detectable if $H^+ \to c\bar{s}$ decays dominate [36] or by a careful study of the details of the final state in $H^+ \to \tau\nu$ decays [37]. We have not considered these possibilities in this paper.

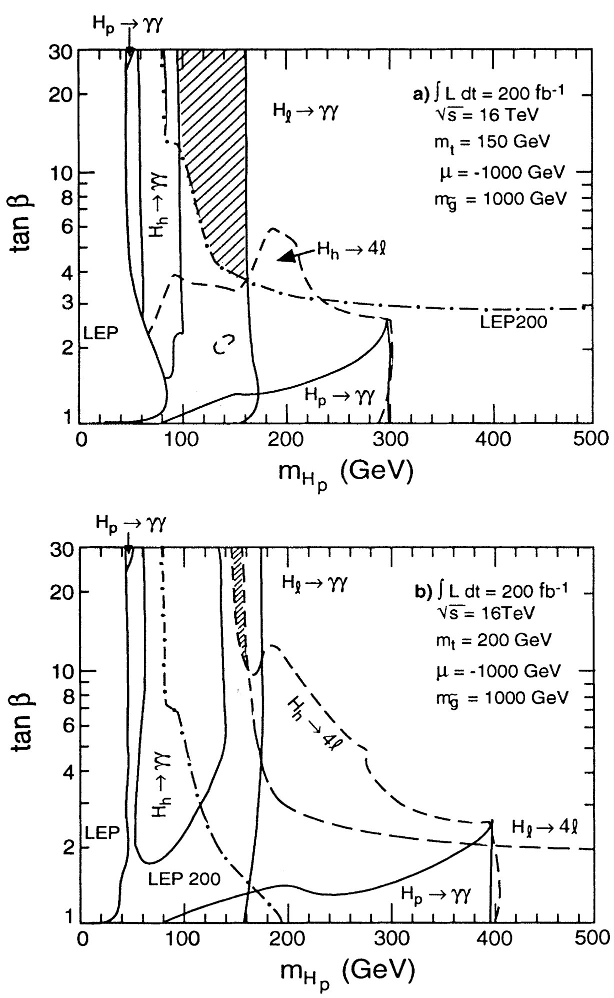

FIG. 6. Same as Fig. 3, except we evaluate for the LHC energy $\sqrt{s} = 16$ TeV and integrated luminosity of 200 fb^{-1}. We show contours for (a) $m_t = 150$ and (b) 200 GeV.

We now consider the prospects for discovering MSSM Higgs bosons at the LHC. We have redone the analysis shown in Fig. 3 and Fig. 4 but for a machine energy, $\sqrt{s} = 16$ TeV. Our results are shown in Fig. 6 for (a) $m_t = 150$ GeV, and (b) $m_t = 200$ GeV. For brevity, we have shown these only for an integrated luminosity of 200 fb^{-1}, corresponding to running the LHC at the high design luminosity option for two years. We see that the qualitative features of Figs. 6(a) and 6(b) closely parallel those of Figs. 3(b) and 4(b). We thus conclude that if the LHC can be operated at a luminosity of 10^{34} $\mathrm{cm}^{-2}\,\mathrm{sec}^{-1}$, it will, after just two years, probe only a slightly smaller region of parameter space as the SSC (operating at an order of magnitude lower luminosity) would in five years. We remark that the region where $t \to H^+ b$ decays should be similar at the LHC and the SSC. In view of the simplifying assumptions that led to (7b) and (7c), we did not deem it necessary to show the $\Delta R_{\tau,\mu} < 0.15$ region separately.

To sum up, we have delineated the regions of parameter space where the signals from the various Higgs bosons of the MSSM might be detectable at the SSC (Figs. 3–5) and at the LHC (Figs. 5 and 6), assuming that their decays into charginos and neutralinos are absent. The impact of these decays on this analysis forms the subject of Sec. III.

III. EFFECT OF SUSY DECAYS ON MSSM HIGGS BOSON SEARCHES

The purpose of this section is to study whether decays of MSSM Higgs bosons into charginos and neutralinos have a significant impact on the detectability of the various signals discussed in Sec. II. We are motivated to consider this possibility because the supersymmetric decay modes of Higgs bosons can occur at large rates (and even be the dominant decay modes) in certain regions of MSSM parameter space. For instance, the SUSY decay modes, which occur via gauge couplings, may dominate SM final states such as $H \to b\bar{b}$ (which takes place via Yukawa interactions), or $H \to WW$ or ZZ (where couplings are suppressed due to mixing-angle factors). Thus, for values of parameters, where $b\bar{b}$ or WW and ZZ are the main SM decay modes, SUSY decays of Higgs bosons may be very important. The branching fractions for the SUSY decays of Higgs bosons were first systematically studied in Refs. [28] and [40], but without the effects of the radiative corrections from top Yukawa interactions incorporated.

We begin by considering the branching fractions for decays of Higgs bosons into charginos and neutralinos. The branching fractions for $H \to$SUSY particles are shown in the μ vs $\tan\beta$ plane in Fig. 7 for (a) H_l, (b) H_h, (c) H_p, and (d) $H^\pm$. In this figure, we have fixed $m_{H_p} = 200$ GeV, $m_{\tilde{g}} = 400$ GeV, $m_{\tilde{q}} = 1000$ GeV, and $m_t = 150$ GeV. The branching fraction for SUSY decays of H_h,

H_p, and $H^\pm$ will generally increase if m_{H_p} increases or $m_{\tilde{g}}$ decreases from our default choices. The region already excluded by LEP experiments is blacked out in Fig. 7. Finally, the region in between the dashed lines is where $m_{\widetilde{W}_1} < 90$ GeV, and is the region capable of being probed at LEP 200; if the MSSM parameters are outside this region, then $\widetilde{Z}_1\widetilde{Z}_2$ production may be the only SUSY signal observable at LEP 200. We also see from Fig. 1 that Higgs bosons searches at LEP 200 should lead to a detectable signal for $\tan\beta < 2-3$, although this conclusion is rather sensitive to the t-quark mass. The following features are worth noting.

(i) As expected, SUSY decays of H_l are strongly suppressed except for values of μ close to the boundary of the region excluded by LEP. Nevertheless, it is instructive to note that up to 70% of the decays of even the lighter scalar may be into SUSY modes for values of parameters allowed by LEP. This, of course, means that its total width correspondingly increases, so that the branching fraction for its only detectable decays in Figs. 3 and 4 are significantly reduced. It should be noted that over much of this region H_l decays only via $H_l \to \widetilde{Z}_1\widetilde{Z}_1$, so that its decays are invisible [28]. There are, however, regions of SUSY parameters, where the potentially visible decay, $H_l \to \widetilde{Z}_1\widetilde{Z}_2$ is also significant. Finally, we see from Fig. 7(a) that if charginos are not observed at LEP 200, the SUSY decays of H_l will be inconsequential, at least for our choice of $m_{\tilde{g}}$ and m_t.

(ii) Turning to the heavier Higgs bosons, we see that their branching fractions into SUSY modes can be very substantial for a large part of the allowed region so that their observable signals shown in Figs. 3, 4, and 5 will again be significantly reduced. As an example, for $\mu = -100$ GeV and $3 < \tan\beta < 8$, the $4l$ signal from H_h decays is reduced to less than 30% of its magnitude in the absence of SUSY decays. The reduction in the $H_p \to \gamma\gamma$ signal and the $t \to bH^+ \to b\tau\nu$ signal is qualitatively similar. We note that unlike the case of H_l, the branching

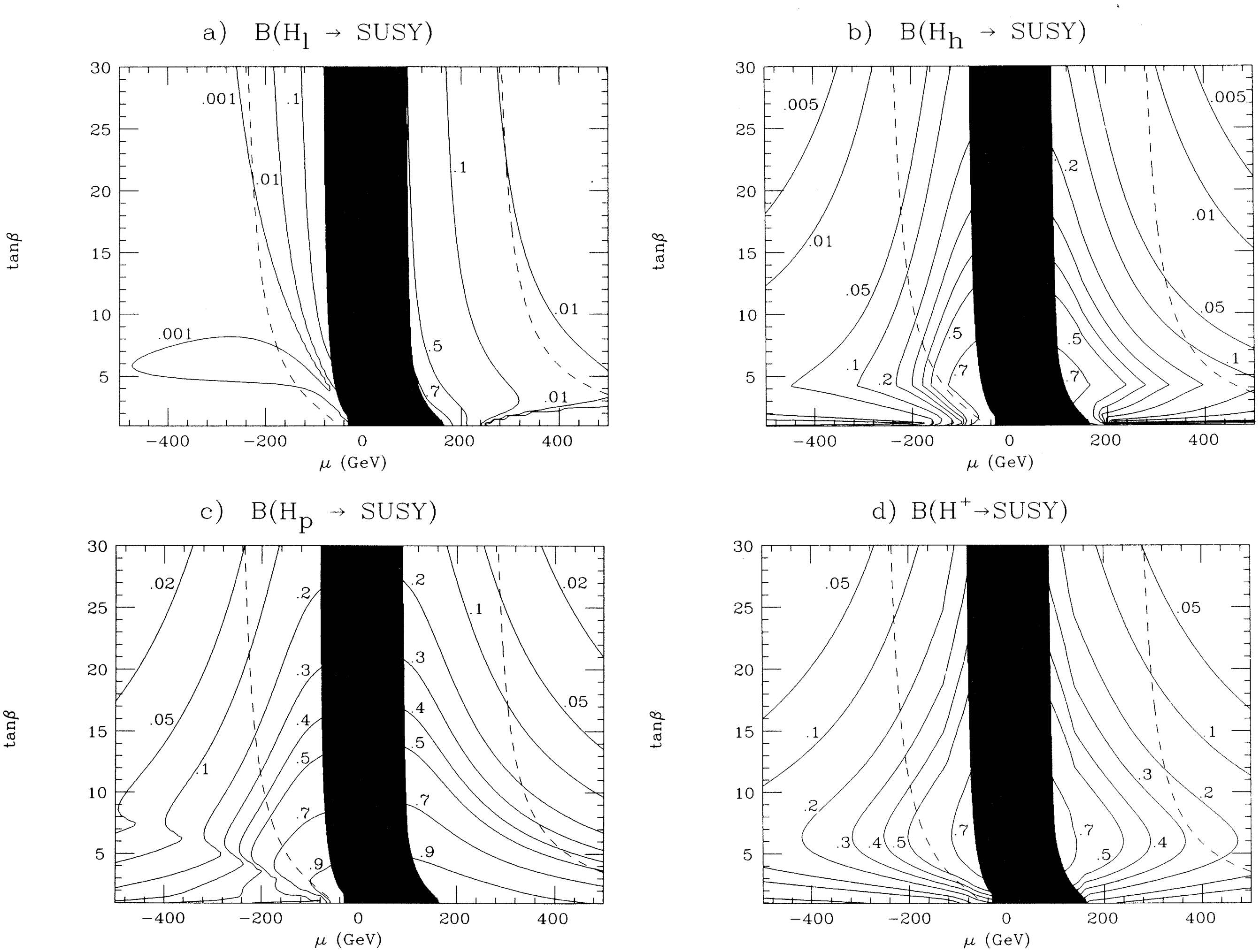

FIG. 7. Branching fractions for (a) $H_l \to$SUSY, (b) $H_h \to$SUSY, (c) $H_p \to$SUSY, and (d) $H^+ \to$SUSY, in the μ vs $\tan\beta$ plane, for $m_{H_p} = 200$ GeV. The blacked out region is excluded by LEP constraints. The region between the dashed lines corresponds to the approximate reach of LEP 200. We have taken $m_{\tilde{g}} = 400$ GeV and $m_t = 150$ GeV.

fractions for the heavier Higgs bosons to decay into $\widetilde{W}_1$ and $\widetilde{Z}_2$ may be quite substantial. Whether these decays lead to observable signals forms the subject of the next section.

(iii) It is interesting to see that there is a significant region of parameter space (near $\mu = -150$ GeV) that appears inaccessible at LEP 200 and where the SUSY branching fractions of H_h, H_p, and $H^{\pm}$ are all in excess of 40 – 50%. For positive values of μ, such a region is present only for the decays of H_p.

(iv) The SUSY decay modes are especially likely to obscure the detection of H_p, which, as we saw in Figs. 3 and 4 was possible [10] only for the $\gamma\gamma$ mode for $\tan\beta = 1$–3; here, the $H_p b\bar{b}$ coupling (despite the $\tan\beta$ enhancement) is still small compared to the gauge coupling that mediates the SUSY decays of H_p. This is the reason the SUSY branching fractions in Fig. 7(c) are quite large (even for rather large values of $|\mu|$ when $\tan\beta$ is close to unity.

In order to illustrate the impact of the SUSY decays of Higgs bosons on the observability of their signals at the SSC we have, as in Figs. 3 and 4, mapped out regions of the m_{H_p}-$\tan\beta$ plane, where the various Higgs bosons signals are observable according to the same criteria, but for the case where the decays to charginos and neutralinos are not so strongly suppressed. This is shown in Figs. 8 and 9 for $m_t = 150$ GeV and $m_t = 200$ GeV, respectively, and for an integrated luminosity of (a) 10 fb^{-1} and (b) 50 fb^{-1}. We have fixed $m_{\tilde{g}} = 400$ GeV and $\mu = -100$ GeV, which is well outside the region probed by LEP or the Tevatron. In our analysis, we have assumed for simplicity that the region of parameter space that can be probed at LEP 200 is unaltered, i.e., the decays of Higgs bosons to charginos and neutralinos will lead to clear signals. This should, of course, be independently studied, since it is possible that H_l decays invisibly to $\widetilde{Z}_1\widetilde{Z}_1$, or that if $H_l \to \widetilde{W}_1\widetilde{W}_1$, the $\widetilde{W}_1$ and $\widetilde{Z}_1$ are rather close in mass so that the visible decay products are not energetic enough for detection.

Comparing Fig. 8 (Fig. 9) with Fig. 3 (Fig. 4), we observe the following.

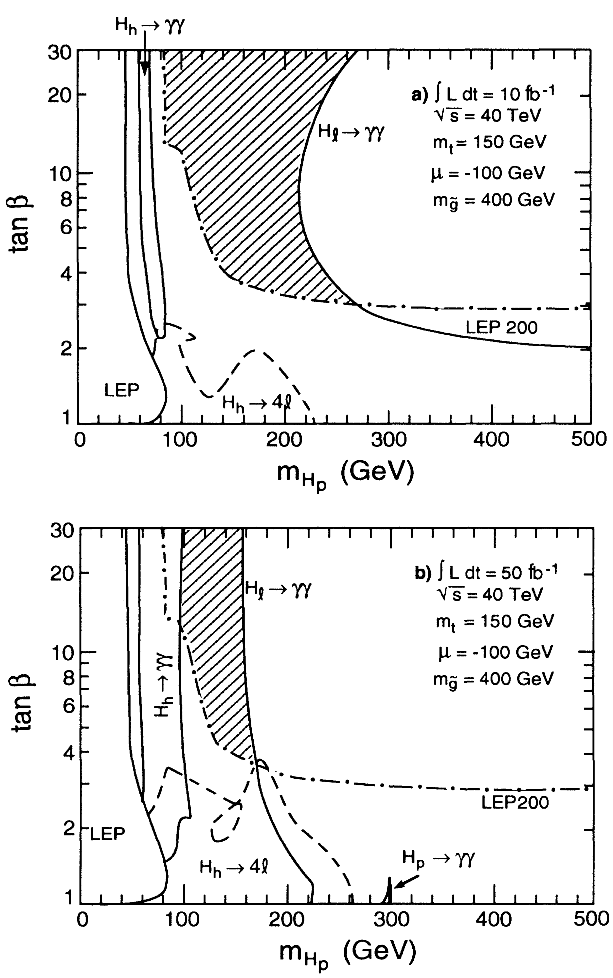

FIG. 8. Same as Fig. 3, except that we have taken $m_{\tilde{g}} = 400$ GeV and $\mu = -100$ GeV, so that many SUSY decay modes of the Higgs bosons are allowed.

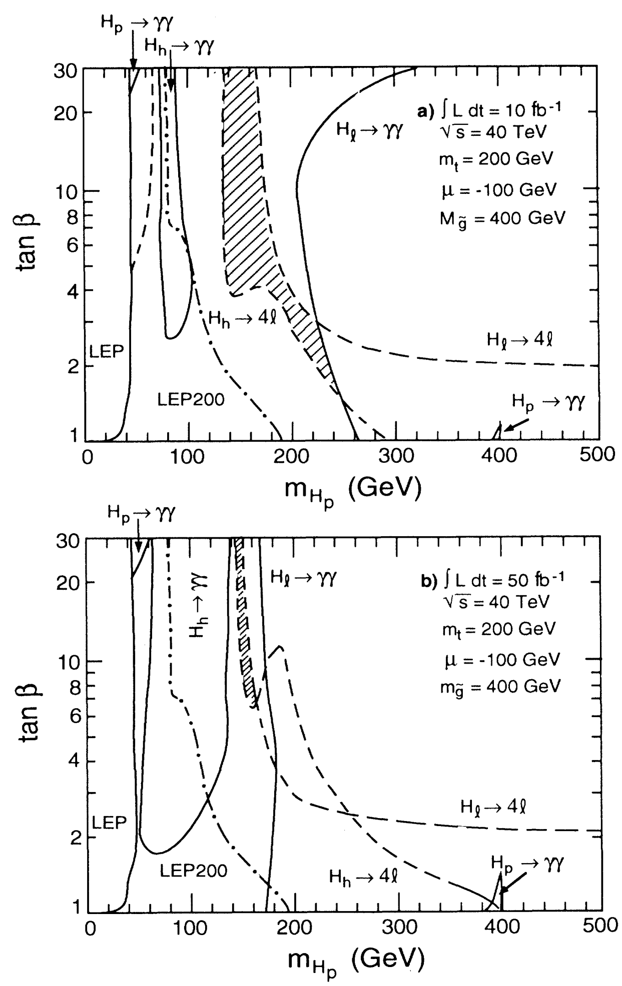

FIG. 9. Same as Fig. 4 ($m_t = 200$ GeV) except that we have taken $m_{\tilde{g}} = 400$ GeV and $\mu = -100$ GeV so that many SUSY decay modes of the Higgs bosons are allowed.

(1) The shaded region where *none* of the usual signals for the MSSM Higgs bosons are observable can be considerably larger if SUSY decays of Higgs bosons are allowed. We remark, however, that a light chargino and neutralino sector, which can enlarge the "hole," will also be more likely to be light enough for detection at LEP 200.

(2) The region where the $H_p \to \gamma\gamma$ signal was observable all but disappears even for five years of operation of the SSC.

(3) The regions of observability of the $H_l \to \gamma\gamma$ signal shrinks noticeably. This is for two reasons. The obvious one is the increased total width from the SUSY decays. In addition there may be a significant negative interference that becomes important when the contribution of the chargino loops to $H_l \to \gamma\gamma$ decays becomes important. The relative importance of these two effects is parameter dependent. The $H_l \to 4l$ contours for $m_t = 200$ GeV are essentially unaltered, since the H_l width is not significantly increased in this case.

(4) Turning to the detectability of H_h, we see that, whereas there is a modest reduction of the $H_h \to \gamma\gamma$ region, the range of parameters where the $4l$ signal is detectable is considerably reduced. This is because near the right-hand boundary of this latter region m_{H_h} is quite large so that the SUSY channels have little phase-space suppression.

(5) We see from Fig. 9(b) that, for a very heavy top quark, signals are detectable for essentially all values of parameters. At present, however, it appears [41] that m_t is likely to be around $140-150$ GeV so that Figs. 3 and 8 are better representatives of the current situation.

(6) Finally, we remark that the size of the shaded region in which there are no observable signals is not the only major issue. As mentioned above, the simultaneous detection of more than one Higgs particle may be necessary before a detection of a nonminimal Higgs sector can be claimed. If SUSY decays of Higgs bosons occur at a large rate, this may become a much more formidable task, at least using the usual detection methods.

The corresponding situation for the LHC is illustrated in Fig. 10 for (a) $m_t = 150$ GeV, and (*b*) $m_t = 200$ GeV. Once again, we have only shown the results for an integrated luminosity of 200 fb^{-1}. A comparison with Fig. 6 shows that the qualitative changes from varying SUSY parameters and masses are the same at the SSC and the LHC. As before, we see that for the $m_t = 200$ GeV case, there is only a very tiny region where there is no observable signal from any of the neutral Higgs bosons, whereas, for the $m_t = 150$ GeV case, the size of this region is increased. We should stress though that the results presented in Figs. 3–10 are dependent upon our optimistic assumptions about the capabilities of the detectors. It is necessary to keep this in mind when drawing general conclusions about the observability of the signals.

We now turn to a study of the effect of the SUSY decays (primarily $H^\pm \to \widetilde{W}_1\widetilde{Z}_1$) on the detectability of the τ signal from the decay of charged Higgs bosons produced via $t \to bH^+$. This was studied in Sec. II, where the region of observability in the m_{H_p} vs $\tan\beta$ plane was mapped out [assuming Eq. (7b) as the limit of observability] by the solid line in Fig. 5. The dashed line shows how this region would shrink if SUSY decays of H^+ are accessible. We have shown this for $m_{\tilde{g}} = 400$ GeV, but have taken $\mu = -70$ GeV (rather than $\mu = -100$ GeV) to increase the impact on the H^+ signal. Of course, charginos are then just beyond the reach of LEP. The region where the decay $H^+ \to \widetilde{W}_1\widetilde{Z}_1$ is kinematically forbidden is also shown. We see that even for this rather contrived choice of parameters, the effect on the region where H^+ was detectable is rather small for $m_t = 150$ GeV, though somewhat larger for a very heavy t quark. We note that if the decay chain $t \to bH^+$, $H^+ \to \widetilde{W}_1\widetilde{Z}_1$ constitutes the main decay mode of the top quark, it could have a dramatic impact on top detection at the Tevatron. While the visible products from the top decay are essentially the same as in the SM, the lepton or jets from $\widetilde{W}_1$ decay can be considerably softer (especially if $m_{\widetilde{W}_1} - m_{\widetilde{Z}_1}$ is small) than those from the decay of the W boson, and so, may fail to pass the experimental cuts imposed to extract the top signal.

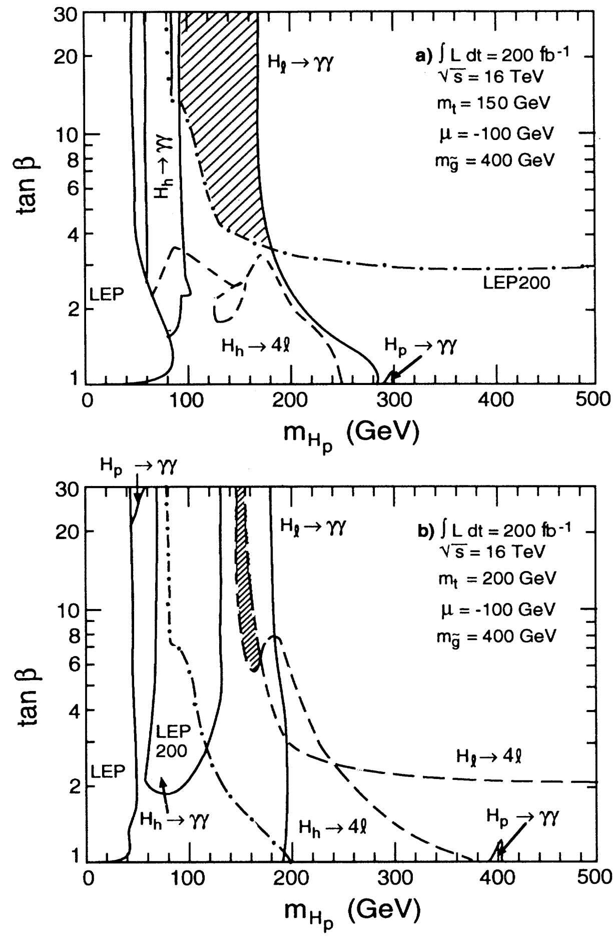

FIG. 10. Same as Fig. 5 (LHC energy) except that we have taken $m_{\tilde{g}} = 400$ GeV and $\mu = -100$ GeV, so that many SUSY decay modes of the Higgs bosons are allowed.

To sum up, we have seen that there are regions of SUSY parameter space that are allowed by all existing experimental constraints, for which the branching fractions for the decays of MSSM Higgs bosons into charginos and neutralinos is substantial, so that the cross sections for the usual signals by which these Higgs bosons might be detected at hadron colliders are reduced. As a result, the region of parameter space where there is no detectable signal can become larger. Almost as important is the fact that the range of parameters where more than one of the Higgs bosons leads to an observable signal is significantly reduced. In particular, the SUSY decays may vitiate any possibility of the detection of H_p, even with our rather optimistic assumptions of the capabilities of the detector. A study of whether the SUSY decay modes lead to new observable effects forms the subject of the next section.

IV. SIGNALS FROM SUPERSYMMETRIC DECAY MODES OF HIGGS BOSONS

One effect of supersymmetric decay modes of Higgs bosons is to reduce rates for conventional signatures. One can, however, also examine whether decays of Higgs bosons into supersymmetric particles can result in *new* detection signatures. Purely hadronic decay modes of Higgs bosons have large backgrounds from multijet production, while mixed leptonic-hadronic decay modes have large backgrounds from heavy flavor (including $t\bar{t}$) production. For this reason, we will concentrate in this section upon examining only the most promising signatures, involving purely leptonic final states. Since single charged lepton final states of Higgs boson decays have large backgrounds from $W \to l\nu$ and $\tau\nu$, we focus here on multicharged-lepton final states. In this section, to be specific, we focus mainly on results for SSC energy ($\sqrt{s} = 40$ TeV); similar analyses would hold for LHC energies.

A. Dilepton $+\not{E}_T$ signatures

The dilepton signal dominantly arises from

$$H_{p,h} \to \widetilde{Z}_2\widetilde{Z}_1 \to l\bar{l}\widetilde{Z}_1\widetilde{Z}_1 \tag{8a}$$

and

$$H_{p,h} \to \widetilde{W}_1\overline{\widetilde{W}}_1 \to l\bar{l}\nu\bar{\nu}\widetilde{Z}_1\widetilde{Z}_1. \tag{8b}$$

There are, in addition, other sources of dileptons from $H_{p,h} \to$SUSY; they tend to be subdominant, and we neglect them for simplicity.

The leptons from the decay of $\widetilde{Z}_2$ in (8a) are always of the same flavor. Furthermore, they are kinematically constrained to satisfy $m(l\bar{l}) < m_{\widetilde{Z}_2} - m_{\widetilde{Z}_1}$. These features can be useful in separating signal from background. In contrast, the lepton pairs from (8b) are generally expected to have a broad invariant mass distribution which only cuts off at $m_{H_{p,h}} - 2m_{\widetilde{Z}_1}$; unlike neutralino decays, the dilepton pairs from charginos can occur with mixed flavors, e.g., $e^{\pm}\mu^{\mp}$.

We show in Fig. 11 (Fig. 12) the cross section for dilepton events at $\sqrt{s} = 40$ TeV from H_p (H_h) decays vs (a) μ, for $m_{H_p} = 200$ GeV, and vs (b) m_{H_p}, for $\mu = -150$ GeV.

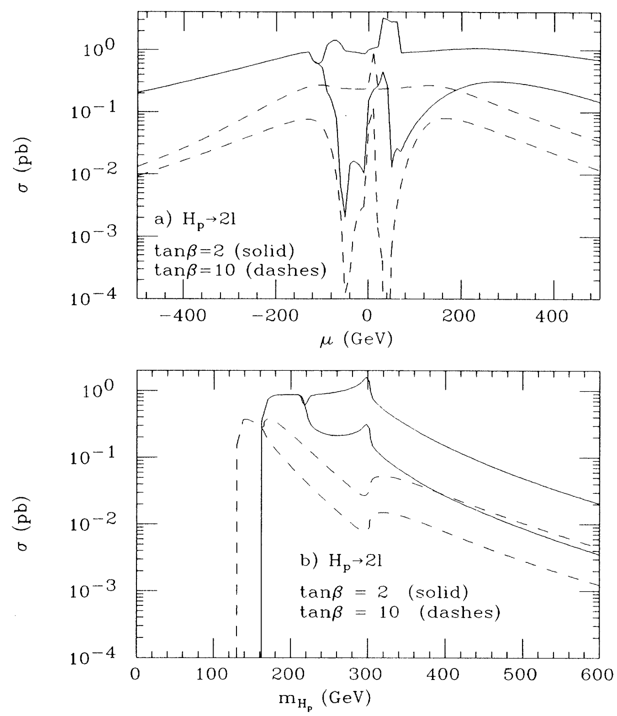

FIG. 11. Total cross sections for dilepton production from decays of H_p to charginos and neutralinos (a) vs μ for $m_{H_p} = 200$ GeV and vs (b) m_{H_p} for $\mu = -150$ GeV, for $\tan\beta = 2$ and 10. The lower curve is dilepton production from the decay $H_p \to \widetilde{Z}_1\widetilde{Z}_2$, while the upper curve is for the sum of $H_p \to \widetilde{Z}_2\widetilde{Z}_1$ and $H_p \to \widetilde{W}_1\overline{\widetilde{W}}_1$. We have also taken $m_{\tilde{g}} = 400$ GeV, $m_{\tilde{q}} = 1000$ GeV and $m_t = 150$ GeV.

We have fixed $m_{\tilde{g}} = 400$ GeV, $m_{\tilde{q}} = m_{\tilde{l}} = 1000$ GeV, and $m_t = 150$ GeV in these figures. We show curves for $\tan\beta = 2$ (solid) and $\tan\beta = 10$ (dashes). The lower curve is due only to reaction (8a), while the upper curve shows the summed cross section from (8a) and (8b).

The dominant SM background to hadronically quiet dilepton events [42] is from W pair production. The WW cross section is about 100 pb at SSC energy, which would yield ~10 pb of cross section for $l^+l'^- + \not{E}_T$ events, where $l, l' = e$ or μ. There would also exist a background from direct continuum production of chargino and neutralino pairs [43,44]. We show in Fig. 13 the dilepton background from (a) $pp \to \widetilde{Z}_1\widetilde{Z}_2$ and (b) $pp \to \widetilde{W}_1\overline{\widetilde{W}}_1$ vs μ for the same parameters as in Figs. 11 and 12.

From Fig. 11, we note that the dilepton signal from $H_p \to \widetilde{Z}_2\widetilde{Z}_1$ sometimes dominates that from $H_p \to \widetilde{W}_1\overline{\widetilde{W}}_1$ and can range up to the 1-pb level, resulting in $\sim 10^4$ events per year at the SSC. From Fig. 12, we see that the dilepton contribution from H_h decay only ranges up to ~0.2–0.5 pb. The SUSY background from Fig. 13 is much larger than signal only when $\mu \sim 0$, which is in the LEP-excluded region (see Fig. 2). Outside the LEP-excluded region, the background from $\widetilde{Z}_1\widetilde{Z}_2$ is frequently negligible, whereas the background from $\widetilde{W}_1\overline{\widetilde{W}}_1$ can range up to the several pb range, making detection of

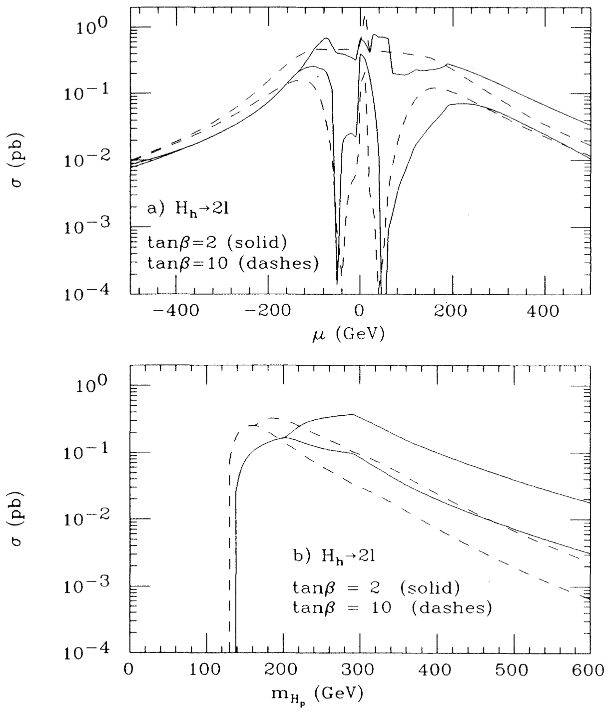

FIG. 12. Same as Fig. 11, except for H_h decays to dileptons via SUSY particles.

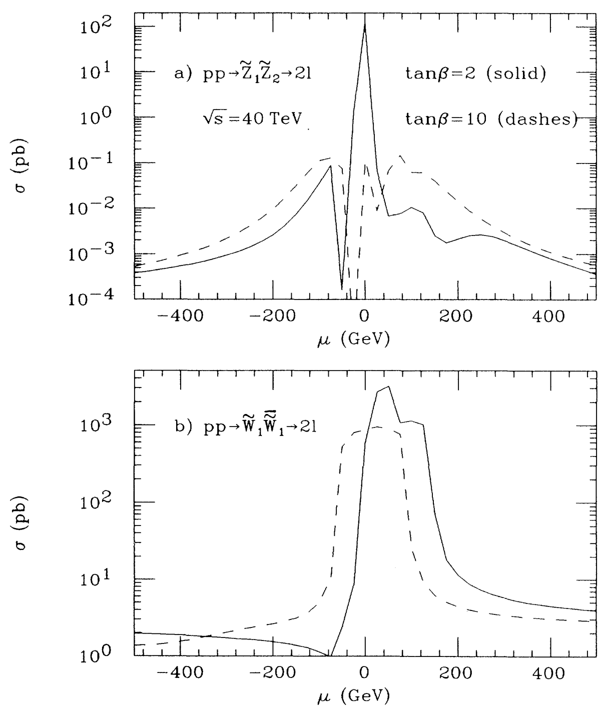

FIG. 13. Cross sections for dilepton production from direct production of (a) $\widetilde{Z}_2\widetilde{Z}_1$ and (b) $\widetilde{W}_1\overline{\widetilde{W}}_1$, at SSC energy, for $\tan\beta = 2$ and 10 vs μ for the same parameters as in Figs. 11 and 12.

a signal difficult. The dilepton invariant mass distribution from chargino pairs, as well as from W pairs, would be spread over a large range of values, whereas the distribution from $\widetilde{Z}_2$ decay would be bounded by $m_{\widetilde{Z}_2} - m_{\widetilde{Z}_1}$. We conclude that discovery of Higgs decays to SUSY particles would be difficult in the dilepton channel, although perhaps some distortion of the low end of the $m(l\bar{l})$ distribution could be measured, which might add confirmatory evidence to a signal in a more promising channel.

B. Four-lepton + $\not{E}_T$ signatures

Next, we turn to the prospects for detecting the MSSM Higgs bosons via the four-lepton decay modes:

$$H_{p,h} \to \widetilde{Z}_i\widetilde{Z}_j \to l\bar{l}\widetilde{Z}_1 + l'\bar{l}'\widetilde{Z}_1. \quad (9)$$

The major supersymmetric background comes from the continuum production of neutralinos, e.g., $\widetilde{Z}_2\widetilde{Z}_2$ production. Within the SM, ZZ production is the dominant source of hadronically quiet $4l$ events. However, ZZ events have very little associated $\not{E}_T$; furthermore, the Z mass reconstruction can also be used as a veto on this background. Assuming ZZ events are distinguishable from $4l$ events from neutralino pairs, $4W$ production is the dominant SM background. The cross section $\sigma(4W)$ depends on the Higgs sector, but is smaller than ~ 20 fb [45] at SSC energy, so that we expect < 0.1 $4l$ events per year from this source.

The expectation for the total number (i.e., without any corrections for detection efficiencies) of $4l$ events per 10^4 pb^{-1} at SSC energy from the $\widetilde{Z}_2\widetilde{Z}_2$ decays of H_p and H_h is shown in Fig. 14 and Fig. 15, respectively, in (a) the μ-$\tan\beta$ plane for $m_{H_p} = 200$ GeV, and (b) m_{H_p}-$\tan\beta$ plane for $\mu = -180$ GeV. These parameters roughly maximize the signal. The remaining parameters are chosen to be $m_{\tilde{g}} = 400$ GeV, $m_{\tilde{q}} = m_{\tilde{l}} = 1000$ GeV, and $m_t = 150$ GeV. The blacked out area corresponds to the region already excluded by experiments at LEP as discussed earlier.

We see that there are substantial regions of the parameter space where the total signal exceeds 10–20 events per year, with the maximum ranging up into the hundreds. The cross section for the *continuum* production $pp \to \widetilde{Z}_2\widetilde{Z}_2 \to l\bar{l}\widetilde{Z}_1 l'\bar{l}'\widetilde{Z}_1$ of $4l$ events is shown vs μ in Fig. 16. We have chosen $m_{\tilde{g}} = 400$ GeV, $m_{\tilde{q}} = m_{\tilde{l}} = 1000$ GeV and illustrated the result for $\tan\beta = 2$, 5, and 30. Except for the spike at $\mu \sim 0$, which is in the LEP excluded region, continuum production of $\widetilde{Z}_2$ pairs generally leads to $\lesssim$ 10–20 events per year at SSC energy. We note, however, that unlike $\widetilde{Z}_2$ pair production via decays of Higgs bosons, continuum production of $\widetilde{Z}_2$ pairs is sensitive to the value of $m_{\tilde{q}}$ for those values of MSSM parameters for which $\widetilde{Z}_2$ is dominantly a gaugino (so that its coupling to Z^0 is suppressed). This occurs for large values of μ and is illustrated in Fig. 16 by the solid curve, where $m_{\tilde{q}} = 410$ GeV and $\tan\beta = 2$. We see that the $4l$ background can be much enhanced or suppressed, so that a measurement of the rate of $4l$ events will be insufficient to deduce the existence of $\widetilde{Z}_2\widetilde{Z}_2$ decays of MSSM Higgs bosons.

Returning to Figs. 14 and 15, we observe the following.

(a) Over much of the parameter space, where the $4l$ cross sections from H_p and H_h decay are largest, there should be some other observable signals at LEP 200. An exception is the large $\tan\beta$ region in Fig. 14(b).

(b) The clustering of the contours near m_{H_p}=200 GeV in Fig. 14(b) and Fig. 15(b) is due to the fact that for smaller values of m_{H_p}, $\widetilde{Z}_2\widetilde{Z}_2$ decays are kinematically forbidden.

(c) The $4l$ events from decays of Higgs bosons to $\widetilde{Z}_2\widetilde{Z}_2$ fill part of the "hole" in the m_{H_p}-$\tan\beta$ plane [see the shaded region of Fig. 3(a)] for which there were no observable conventional signals. However, the hole is not completely filled because for our choice of parameters,

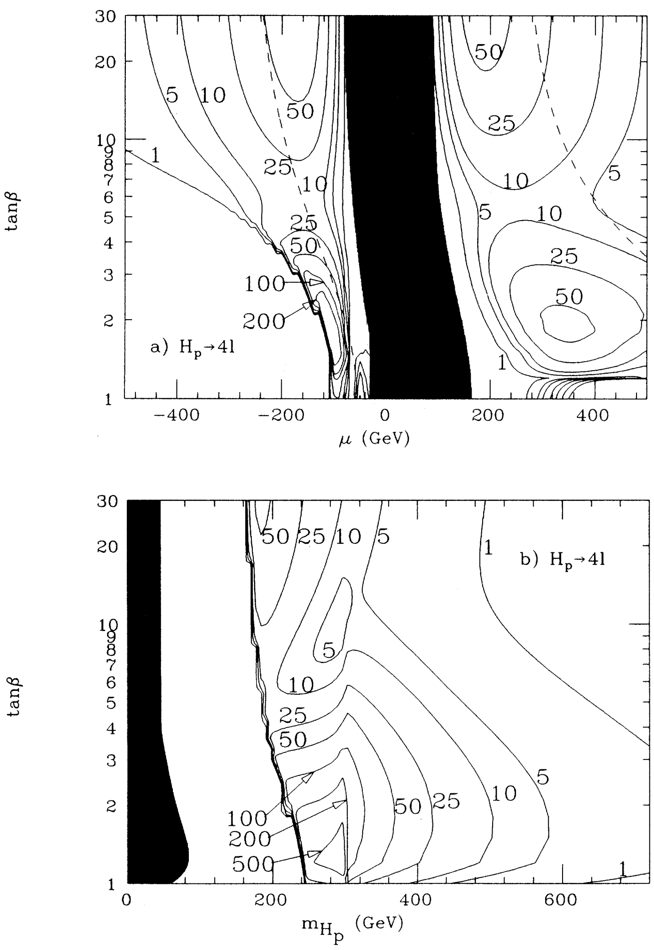

FIG. 14. Contour plots of number of $H_p \rightarrow \widetilde{Z}_2\widetilde{Z}_2 \rightarrow 4l + \not{E}_T$ events per year at SSC energy assuming integrated luminosity of 10^4 pb^{-1}, (a) in the μ vs $\tan\beta$ plane for m_{H_p} = 200 GeV, and (b) in the m_{H_p} vs $\tan\beta$ plane for μ = −180 GeV. We have also taken $m_{\tilde{g}}$ = 400 GeV and m_t = 150 GeV. The blacked out region is excluded by LEP constraints. The region between the dashed lines in (a) corresponds to the approximate reach of LEP 200.

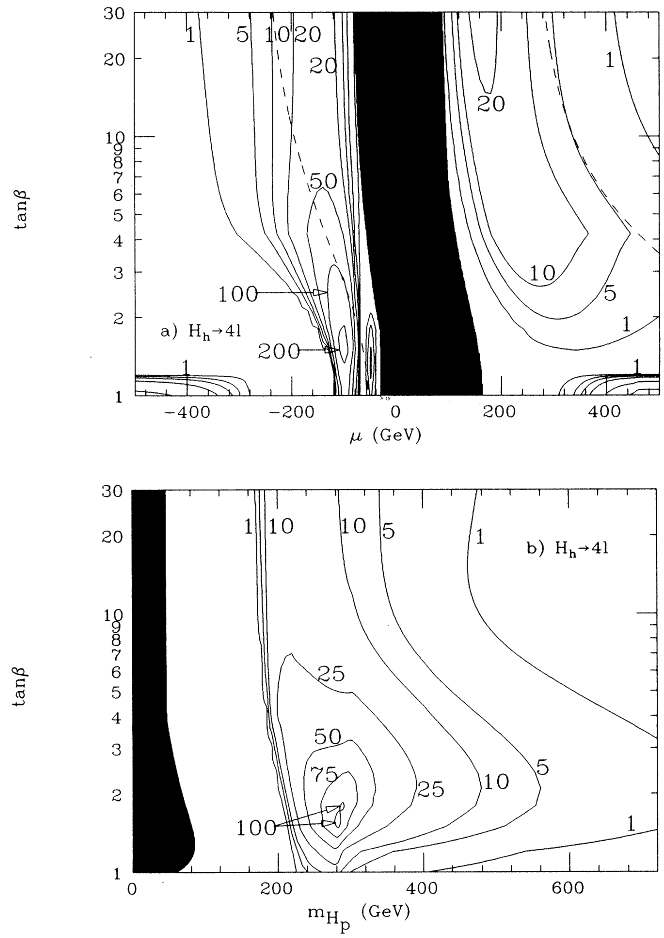

FIG. 15. Same as Fig. 14, except for $H_h \rightarrow \widetilde{Z}_2\widetilde{Z}_2 \rightarrow 4l + \not{E}_T$.

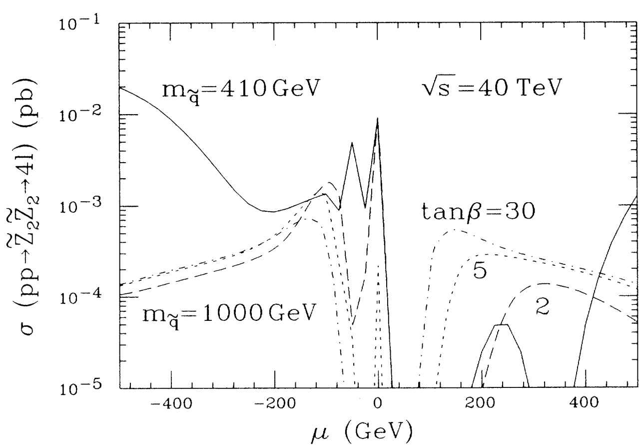

FIG. 16. Plot of cross section in pb for $pp \rightarrow \widetilde{Z}_2\widetilde{Z}_2 \rightarrow 4l + \not{E}_T$ vs μ for $\tan\beta$ = 2, 5, and 30 and $m_{\tilde{q}}$ = 1000 GeV (large and small dashed curves and dot-dashed curves) and for $\tan\beta$ = 2 and $m_{\tilde{q}}$ = 410 GeV (solid curve). We take $m_{\tilde{g}}$ = 400 GeV.

$\widetilde{Z}_2\widetilde{Z}_2$ decays are kinematically forbidden for some of the m_{H_p} values inside the shaded region of Fig. 7.

(d) There is a substantial range of parameters for which $4l + \not\!\!E_T$ decay modes of H_p and H_h signals might be observable. Thus SUSY decays extend the regions of parameter space where more than one Higgs boson might be simultaneously observable. A dedicated simulation of the signal is needed, however, before definitive conclusions can be drawn.

We should keep in mind that only total rates are shown for $4l$ events in Fig. 14 and Fig. 15. The actual signal will be reduced once experimental cuts are incorporated. In order to get some idea of the nature of these events, we have shown the p_T distributions of the four leptons (ranked according to p_T) along with the $\not\!\!E_T$ distribution in Fig. 17(a). For illustration, we have taken $m_{H_p} = 250$ GeV, and fixed other parameters to be $m_{\tilde{g}} = 400$ GeV, $m_{\tilde{q}} = m_{\tilde{l}} = 1000$ GeV, $\mu = -100$, $\tan\beta = 2$, and $m_t = 150$ GeV. We see that the fastest lepton almost always has $p_T > 20$ GeV and can therefore be used as a trigger for the signal. The leptons should be centrally produced and well separated in angle, since they come from centrally produced massive scalars or pseudoscalars. We also see from the p_T distribution of the slower leptons that the size of the signal will depend on the detector ability to identify leptons of $p_T \sim 0-20$ GeV in the central region. In the case where one lepton is very soft and not identified, the signal is classified as a $3l$ event. Then the dominant background would be from $3W$ production, which has been estimated [46] to result in $\sim$64 events per year at the SSC. The leptons from W decay should be much harder than those from SUSY decays of Higgs bosons, so that it should be possible to enhance the signal to background by suitable $p_T(l)$ and $\not\!\!E_T$ cuts.

We show in Fig. 17(b) the invariant mass distribution for like-flavor dileptons and all four leptons in $e^+e^-\mu^+\mu^-$ events from $H_p \to \widetilde{Z}_2\widetilde{Z}_2$ decays. These distributions [47] cut off at $m_{\widetilde{Z}_2}-m_{\widetilde{Z}_1}$ and $m_{H_p}-2m_{\widetilde{Z}_1}$, respectively. The endpoints of these distributions will be smeared somewhat by the effects of finite experimental energy resolution. However, if the mass of the Higgs boson can be determined from measuring its $\gamma\gamma$ or ZZ decay modes, then good resolution of the invariant mass distribution limits can allow a precise measurement of the $\widetilde{Z}_2$ and $\widetilde{Z}_1$ mass. This can be very important, since neutralino mass measurement is otherwise very difficult, even at e^+e^- colliders.

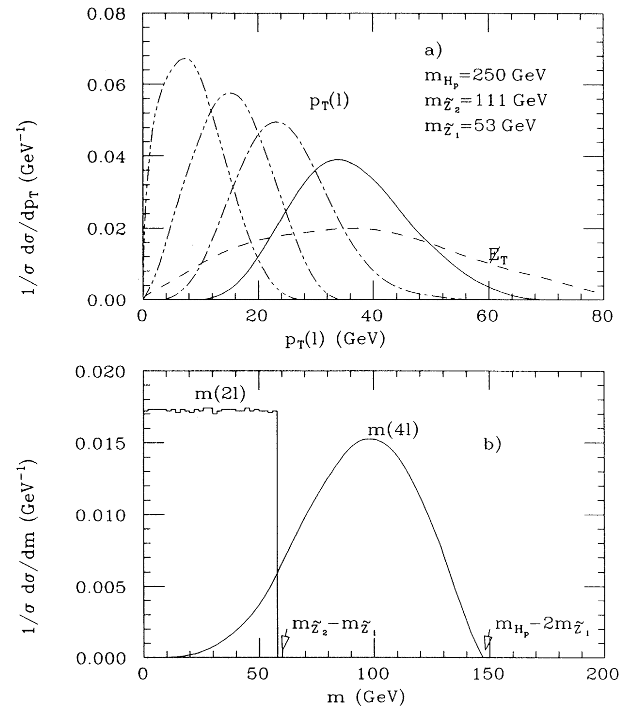

FIG. 17. Plot of distribution in (a) lepton p_T for the four leptons from $H_p \to \widetilde{Z}_2\widetilde{Z}_2 \to 4l + \not\!\!E_T$, where the leptons are ordered from largest to smallest p_T, for $m_{H_p} = 250$ GeV, $m_{\tilde{g}} = 400$ GeV, $\mu = -100$ GeV, and $\tan\beta = 2$. We also show the $\not\!\!E_T$ distribution. In (b), we show like-flavor $m(l\bar{l})$ distribution and $m(4l)$ distribution. If the H_p or H_h mass is known from reconstructing the ZZ or $\gamma\gamma$ mass bumps, then these distributions can help determine the $\widetilde{Z}_2$ and $\widetilde{Z}_1$ masses.

C. Rare decay of $t \to bH^+ \to b + 3l$

In addition to the dilepton and four-lepton signals from the $\widetilde{Z}_1\widetilde{Z}_2$ and $\widetilde{Z}_2\widetilde{Z}_2$ decays of neutral Higgs bosons discussed above, the decay $H^\pm \to \widetilde{W}_1^\pm\widetilde{Z}_2$ can potentially give rise to trilepton decays of the top quark provided the decay $t \to bH^+$ is kinematically allowed. Since hadron supercolliders are essentially top-pair factories, it may be possible to search for these as rare-decay modes of the top quark. As discussed earlier, Felcini [35] has already shown that even with stringent requirements to cleanly tag $t\bar{t}$ events, $\gtrsim 2500$ tagged top events are expected at the LHC for an integrated luminosity of 10 fb^{-1}. We therefore conclude that at the SSC it should be possible to detect rare-decay modes of the top if branching fractions exceed $\sim 10^{-4}$. Toward this end, we have shown in Fig. 18 the region of parameter space where the branching fraction for $t \to bH^+ \to b\widetilde{W}_1\widetilde{Z}_2 \to b + 3l + \not\!\!E_T$ exceeds 10^{-4} and 10^{-3}, for (a) $m_t = 150$ and (b) 200 GeV. As usual, l denotes an e or μ. Here, we have set $m_{\tilde{g}} = 400$ GeV and $m_{\tilde{q}} = 1000$ GeV, while we have also set $\mu = -70$ GeV. For much larger values of $|\mu|$, the charginos and neutralinos become too heavy for the $H^+ \to \widetilde{W}_1\widetilde{Z}_2$ decay to take place. The region to the left of the dot-dashed curve is where no supersymmetric decay modes of H^+ are allowed. The region to the right of the dashed line has a charged-Higgs-boson mass too large for the decay $t \to bH^+$ to occur.

In such top-pair events, the existence of one top would be assured via its decay to $e\mu$ as shown by Felcini; the other would decay to a final state containing $b\widetilde{Z}_1\widetilde{Z}_1 + 3l$. The two $\widetilde{Z}_1$'s would absorb much of the top rest mass energy, resulting in a rather soft trilepton energy spectrum. If detectable, such modes would signal the presence of not only charged-Higgs-boson decays of top quarks, but also a supersymmetric decay of the charged

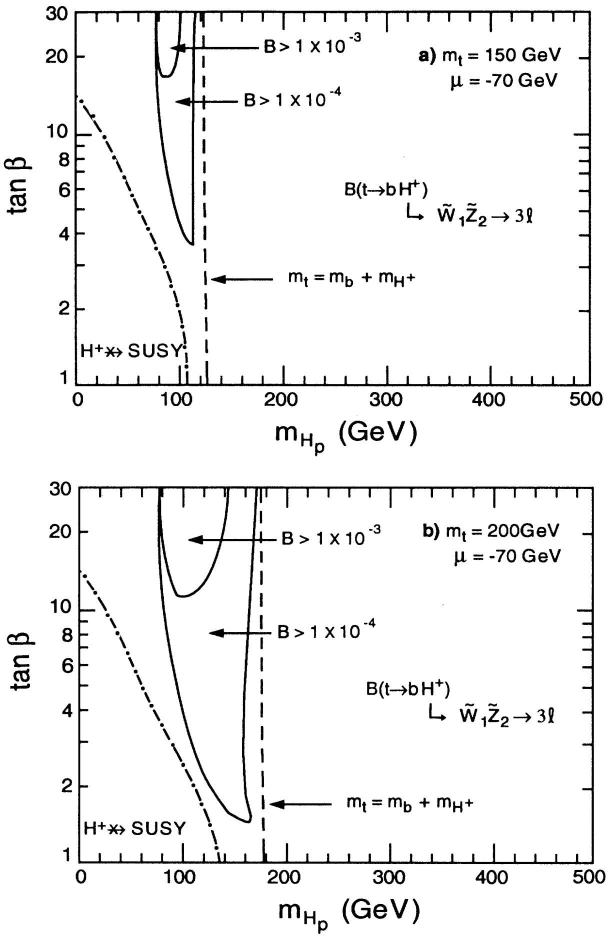

FIG. 18. Contour plot of branching ratios for $t \to bH^+ \to b\widetilde{W}_1\widetilde{Z}_2 \to b + 3l + 2\widetilde{Z}_1$ in the m_{H_p} vs $\tan\beta$ plane, for (a) $m_t = 150$ and (b) 200 GeV. We take $m_{\tilde{g}} = 400$ GeV and $\mu = -70$ GeV. The region to the left of the dot-dashed curve is where $H^+ \to$SUSY particles are not allowed; we also show via the vertical dashed line the phase-space limit for $t \to bH^+$.

Higgs boson. As before, the two leptons from $\widetilde{Z}_2 \to \widetilde{Z}_1 + l\bar{l}$ decay will have $m(l\bar{l}) < m_{\widetilde{Z}_2} - m_{\widetilde{Z}_1}$, while $m(3l) < m_{H^+} - 2m_{\widetilde{Z}_1}$. Hence, if $m_{\widetilde{Z}_2}$ or $m_{\widetilde{Z}_1}$ is known, a mass measurement of H^+ is possible, if a sufficient number of events containing $3l$ are identified.

V. SUMMARY AND CONCLUSIONS

To summarize, in this paper we have made a detailed study of the detectability of Higgs bosons of MSSM, including the case where Higgs bosons decay to charginos and neutralinos are allowed. First, we mapped out regions of MSSM parameter space already constrained by precision data from LEP on Z decays. We found that LEP, and even LEP 200, will not be able to cover the whole MSSM parameter space in the search for Higgs bosons.

Hadron supercolliders such as the SSC and LHC will be able to cover most of the remaining parameter space via the conventional search for $\gamma\gamma$, $l\gamma\gamma$, and $4l$ events. This study was performed in Sec. II, assuming along with many other authors [10, 12, 21–26] that supersymmetric decay modes of Higgs bosons are not allowed. In many of the regions of parameter space, it is possible that more than one Higgs boson can be discovered, although there are also regions where only one Higgs boson may be visible. However, a hole in the parameter space was found, where *none* of the Higgs bosons yields an observable signal.

When working within the framework of the MSSM, it is not a realistic assumption to neglect the possibility of supersymmetric decay modes of Higgs bosons. We show in Sec. III that the branching fractions for the heavier Higgs bosons (H_p, H_h, and $H^{\pm}$) into charginos and neutralinos can be not only substantial, but even dominant, for a wide range of MSSM parameters. This necessitates a reanalysis of Sec. II, when SUSY decay modes are allowed. It is found that when SUSY decay modes of Higgs bosons are allowed, the regions of parameter space where more than one Higgs boson may be visible are decreased. The hole where no Higgs boson is visible also expands, due to the decrease of Higgs boson branching fractions into SM modes. The region where $t \to bH^+ \to b\tau\nu$ is potentially visible decreases as well.

We investigated in Sec. IV whether the SUSY decays of Higgs bosons can lead to *new* modes for detection. It was found to be very difficult to detect H_p or H_h via $2l + \not{E}_T$ final states due to large backgrounds from direct WW and $\widetilde{W}_1\overline{\widetilde{W}}_1$ production. The most promising case for detecting H_p and H_h via SUSY decays is when $H_{p,h} \to \widetilde{Z}_2\widetilde{Z}_2 \to 4l + \widetilde{Z}_1\widetilde{Z}_1$, an analog of the gold-plated $H_{\rm SM} \to ZZ \to 4l$ mode. Over some substantial regions of parameter space, the $4l + \not{E}_T$ mode leads to observable rates if detectors can detect relatively soft isolated leptons. The most dangerous background is direct production of neutralino pairs; however, when the $H_{p,h} \to 4l + \not{E}_T$ signal is large, this background typically occurs at a much smaller rate. The $4l + \not{E}_T$ signal can sometimes fill part of the hole referred to above, but this is not true in general. An interesting ramification of the $4l + \not{E}_T$ mode is that it may allow a mass measurement of the $\widetilde{Z}_2$ and $\widetilde{Z}_1$ particles, if the decaying Higgs particle mass is already measured via its $\gamma\gamma$ or $ZZ \to 4l$ mode; such mass measurements are difficult even in the environment of an e^+e^- supercollider. Finally, it is found that if $t \to bH^+$ decays are allowed, there exist regions of parameter space where a rare decay of $t \to bH^+ \to \widetilde{W}_1\widetilde{Z}_2 \to b + 3l + \not{E}_T$ may be observable, again, if there exists sufficient detection capability for low p_T leptons ($p_T \sim$ 2–10 GeV). This would signal the decay of charged Higgs to SUSY particles, and could conceivably allow an m_{H^+} mass measurement, if one already knows $m_{\widetilde{Z}_1}$.

In an analysis such as the present one, where one must explore a multidimensional parameter space, one must select a limited number of parameter choices of the MSSM; a complete scan of parameter space is not possible. We should mention here that the size of the multilepton signals from supersymmetric decays of Higgs bosons discussed above can be considerably greater than shown in Figs. 11, 12, 14, and 16. To see this, we recall that we have, throughout our analysis, assumed that $m_{\tilde{q}} = m_{\tilde{l}} = m_{\tilde{\nu}}$. It is well known [4, 7], though, that in models with a common sfermion mass at the unification scale, sleptons are considerably lighter than squarks. Ross and Roberts have obtained such a sparticle mass spectrum in a recent analysis [48]. This has important implications for the decays of neutralinos: in particular, if either the parent and daughter neutralinos in the decay $\widetilde{Z}_j \to \widetilde{Z}_i + f\bar{f}$ are dominantly gauginolike, the $Z\widetilde{Z}_i\widetilde{Z}_j$ coupling is suppressed by mixing angles, so that the sfermion exchange contribution to neutralino decay can dominate. If, further, sleptons are much lighter than squarks, the leptonic branching ratios of neutralinos can be substantially enhanced. For our specific case, if $|\mu|$ is very large, $\widetilde{Z}_1$ and $\widetilde{Z}_2$ are both gauginolike, while $\widetilde{Z}_3$ and $\widetilde{Z}_4$ are essentially Higgsinolike; in this case, the $Z\widetilde{Z}_1\widetilde{Z}_2$ coupling is doubly suppressed.

Ross and Roberts find [48], assuming $m_t = 160$ GeV, that $m_{\tilde{g}} \simeq 354$ GeV, $m_{\tilde{q}} \simeq 360$ GeV, $m_{\tilde{l}} \simeq 210$ GeV, $m_{H_p} \simeq 264$ GeV, and $\tan\beta = 21$. For this spectra, by examining Figs. 3 and 6, we find that only one SUSY Higgs should be visible via conventional modes at the SSC and/or LHC: that is the $H_l \to \gamma\gamma$. However, for this spectra, the H_p and H_h can have large branching fractions to charginos and neutralinos, depending on the value of μ. Furthermore, as $|\mu|$ is varied from 100 to 500 GeV, the branching ratio for $\widetilde{Z}_2 \to \widetilde{Z}_1 l\bar{l}$ can vary between near 0 to $\sim$ 30%. In contrast, most of the analysis of this paper has used parameters for which $B(\widetilde{Z}_2 \to \widetilde{Z}_1 l\bar{l}) \sim 6\%$ (due to Z propagator domination of decay modes). Hence, the $2l + \not{E}_T$ signal could be enhanced by a factor of $\sim$5, while the $4l + \not{E}_T$ signal rates could be enhanced by factors of $\sim$25. Of course, signals from continuum neutralino production will be enhanced by similar factors. This should be kept in mind when evaluating the feasibility of the multilepton signals from SUSY decays of Higgs bosons.

ACKNOWLEDGMENTS

We wish to thank F. Zwirner and G. Kane for discussions. X.T. wishes to thank the National Science Foundation's U.S.-Japan cooperative program and the KEK theory group for support. This research was supported in part by the U.S. Department of Energy under Contract Nos. DE-FG05-87ER40319, DE-AM03-76SF00235, and DE-FG05-85ER40200.

[1] J. Gunion *et al.*, in *Research Directions for the Decade*, Proceedings of the Workshop, Snowmass, Colorado, 1990, edited by E. L. Berger and I. Butler (World Scientific, Singapore, 1991); S. L. Wu *et al.*, in *Proceedings of ECFA Workshop on LEP 200*, Aachen, West Germany, 1986, edited by A. Bohm and W. Hoogland (CERN Report No. 87-08, Geneva, Switzerland, 1987), Vol. 2, p. 312; in *Z Physics at LEP*, Proceedings of the Workshop, Geneva, Switzerland, 1989, edited by G. Altarelli, R. Kleiss, and C. Verzegnassi (CERN Yellow Report No. 89-08, Geneva, 1989), Vol. 2; V. Barger, K. Cheung, B. A. Kniehl, and R. J. N. Phillips, Phys. Rev. D **46**, 3725 (1992).

[2] S. L. Wu, in *The Vancouver Meeting — Particles and Fields '91*, Proceedings of the Joint Meeting of the Division of Particles and Fields of the American Physical Society and the Particle Physics Division of the Canadian Association of Physicists, Vancouver, 1991, edited by D. Axen, D. Bryman, and M. Comyn (World Scientific, Singapore, 1992).

[3] E. Witten, Nucl. Phys. **B185**, 513 (1981); R. Kaul, Phys. Lett. B **109**, 19 (1981); N. Sakai, Z. Phys. C **11**, 152 (1981); S. Dimopoulos and H. Georgi, Nucl. Phys. **B193**, 150 (1981).

[4] For a recent review, see X. Tata, in *The Standard Model and Beyond*, edited by J. E. Kim (World Scientific, Singapore, 1991), p. 304. For a review of the prospects for SUSY searches at LEP and LEP 200, see M. Chen *et al.*, Phys. Rep. **159**, 201 (1988).

[5] For a review of LEP limits, see, e.g., M. Davier, in *Proceedings of the Joint International Lepton-Photon Symposium and Europhysics Conference on High Energy Physics*, Geneva, Switzerland, 1991, edited by S. Hegarty, K. Potter, and E. Quercigh (World Scientific, Singapore, 1992). Hadron collider limits are reviewed by L. Pondrom, in *Proceedings of the 25th International Conference on High Energy Physics*, Singapore, 1990, edited by K. K. Phua and Y. Yamaguchi (World Scientific, Singapore, 1991), Vol. 1, p. 144.

[6] J. Gunion, H. Haber, G. Kane, and S. Dawson, *The Higgs Hunter's Guide* (Addison-Wesley, Redwood City, CA, 1990).

[7] For a review of the MSSM, see H. P. Nilles, Phys. Rep. **110**, 1 (1984); P. Nath, R. Arnowitt, and A. Chamseddine, *Applied $N = 1$ Supergravity*, ICTP Series in Theoretical Physics, Vol. I (World Scientific, Singapore, 1984); H. Haber and G. Kane, Phys. Rep. **117**, 75 (1985).

[8] Y. Okada, M. Yamaguchi, and T. Yanagida, Phys. Lett. B **262**, 54 (1991); Prog. Theor. Phys. **85**, 1 (1991); H. Haber and R. Hempfling, Phys. Rev. Lett. **66**, 1815 (1991); J. Ellis, G. Ridolfi, and F. Zwirner, Phys. Lett. B **257**, 83 (1991); R. Barbieri, M. Frigeni, and F. Caravaglios, *ibid.* **258**, 167 (1991); A. Yamada, *ibid.* **263**, 233 (1991).

[9] ALEPH Collaboration, D. Decamp *et al.*, Phys. Lett. B **265**, 475 (1991); Phys. Rep. **216**, 253 (1992); DELPHI Collaboration, P. Abreu *et al.*, Phys. Lett. B **245**, 276 (1990); L3 Collaboration, B. Adeva *et al.*, *ibid.* **251**, 311 (1990); **252**, 511 (1990); OPAL Collaboration, M. Akrawy *et al.*, Z. Phys. C **49**, 1 (1991); OPAL Collaboration, P. D. Acton *et al.*, Phys. Lett. B **268**, 122 (1991).

[10] H. Baer, M. Bisset, C. Kao, and X. Tata, Phys. Rev. D **46**, 1067 (1992).

[11] We have checked that the requirement that the branching fraction for the decay $Z \to H_l H_p <$ few $\times 10^{-6}$

(corresponding to a sample of 2 000 000 Z's) essentially coincides with the contour for $m_{H_l} + m_{H_p} = M_Z$ shown in Fig. 1.

[12] Z. Kunszt and F. Zwirner, Report No. CERN-TH.6150/91 (unpublished).

[13] LEP Collaborations, Phys. Lett. B **276**, 247 (1992).

[14] D. Bardin *et al.*, Report No. CERN-TH.5468/89, 1989 (unpublished).

[15] See, e.g., Davier [5].

[16] ALEPH Collaboration, D. Decamp *et al.*, Phys. Lett. B **244**, 541 (1990); Phys. Rep. **216**, 253 (1992); OPAL Collaboration, M. Akrawy *et al.*, Phys. Lett B **248**, 211 (1990).

[17] M. Drees and X. Tata, Phys. Rev. D **43**, 2971 (1991).

[18] We have checked that the excluded region is insensitive to the precise bound on $\Delta\Gamma_Z$ in Eq. (2a) so that our conclusion is independent of any residual systematic errors. Furthermore, the regions excluded by (2a) and (2c) virtually coincide.

[19] Pondrom [5], and contribution by A. Beretvas on behalf of the CDF Collaboration, in H. Baer *et al.*, in *Research Directions for the Decade* [1].

[20] H. Baer, X. Tata, and J. Woodside, Phys. Rev. D **44**, 207 (1991).

[21] J. Gunion and L. Orr, Phys. Rev. D **46**, 2052 (1992).

[22] V. Barger, M. Berger, A. Stange, and R. Phillips, Phys. Rev. D **45**, 4128 (1992).

[23] J. Gunion, R. Bork, H. Haber, and A. Seiden, Phys. Rev. D **46**, 2040 (1992).

[24] J. Gunion, H. Haber, and C. Kao, Phys. Rev. D **46**, 2907 (1992).

[25] C. Kao, Phys. Rev. D **46**, 4907 (1992).

[26] See *Proceedings of the ECFA Large Hadron Collider Workshop*, Aachen, Germany, 1990, edited by G. Jarlskog and D. Rein (CERN Report No. 90-10 Geneva, Switzerland, 1990), Vol. II, Sec. A5.

[27] H. Baer, M. Bisset, X. Tata, and J. Woodside, Phys. Rev. D **46**, 303 (1992).

[28] H. Baer, D. Dicus, M. Drees, and X. Tata, Phys. Rev. D **36**, 1363 (1987); K. Griest and H. Haber, *ibid.* **37**, 719 (1988).

[29] D. Dicus, C. Kao, and W. Repko, Phys. Rev. D **36**, 1570 (1987); N. Glover and J. van der Bij, Nucl. Phys. **B321**, 561 (1989).

[30] J. Gunion, G. Kane, and J. Wudka, Nucl. Phys. **B299**, 231 (1988).

[31] SDC, Letter of Intent, publication SDC-90-00151.

[32] R. Zhu, Caltech Report No. CALT-68-1777, 1992 (unpublished).

[33] W. Marciano and F. Paige, Phys. Rev. Lett. **66**, 2433 (1991); J. Gunion, Phys. Lett. B **261**, 510 (1991).

[34] CDF Collaboration, F. Abe *et al.*, Phys. Rev. D **45**, 3921 (1992).

[35] M. Felcini, in *Proceedings of the ECFA Large Hadron Collider Workshop* [26], Vol. II, p. 414.

[36] R. M. Barnett *et al.*, Lawrence Berkeley Laboratory Report No. LBL-29774, 1990 (unpublished); R. M. Barnett, R. Cruz, J. Gunion, and B. Hubbard, Phys. Rev. D **47**, 1048 (1993).

[37] R. Godbole and D. P. Roy, Phys. Rev. D **43**, 3640 (1991); D. P. Roy, Phys. Lett. B **283**, 403 (1992); **277**, 183 (1992).

[38] R. K. Ellis, I. Hinchliffe, M. Soldate, and J. van der Bij, Nucl. Phys. **B297**, 221 (1988).

[39] L. DiLella, in *Proceedings of the ECFA Large Hadron Collider Workshop* [26], Vol. II, p. 530; (CERN Report No. 90-10, Geneva, 1990) see also K. Bos, F. Anselmo, and B. van Eijk (unpublished).

[40] J. Gunion and H. Haber, Nucl. Phys. **B278**, 449 (1986).

[41] For a recent study, see D. Schaile, Z. Phys. C **54**, 387 (1992).

[42] If m_t is just slightly greater than M_W so that the b jet from the decay $t \to bW$ is soft, $t\bar{t}$ production could be a significant background. In view of the CDF bound [34] and the analysis of [41], we exclude this possibility in this paper.

[43] R. Barbieri, F. Caravaglios, M. Frigeni, and M. Mangano, Nucl. Phys. **B367**, 28 (1991).

[44] For earlier work on gaugino pair production at hadron colliders, see H. Baer, H. Hagiwara, and X. Tata, Phys. Rev. D **35**, 1598 (1987); P. Nath and R. Arnowitt, Mod. Phys. Lett. A **2**, 331 (1987).

[45] V. Barger, T. Han, and H. Pi, Phys. Rev. D **41**, 824 (1990).

[46] V. Barger and T. Han, Phys. Lett. B **212**, 117 (1988).

[47] The distribution is flat because we have assumed a constant matrix element for the decay $\widetilde{Z}_2 \to \widetilde{Z}_1 l\bar{l}$.

[48] G. Ross and R. Roberts, Nucl. Phys. **B377**, 571 (1992); for related work, see R. Arnowitt and P. Nath, Phys. Rev. Lett. **69**, 725 (1992); S. Kelley *et al.*, Report No. CERN-TH.6498/92, 1992 (unpublished).